CHEMISTRY
A EUROPEAN JOURNAL

ChemPubSoc
Europe

DOI: 10.1002/chem.201103203

Aggregation and Supramolecular Membrane Interactions that Influence Anion Transport in Tryptophan-Containing Synthetic Peptides

Megan M. Daschbach,[a] Saeedeh Negin,[a] Lei You,[a] Matthew Walsh,[b] and George W. Gokel*[a, c]

Abstract: Self-assembly is a desired property in supramolecular chemistry, but extensive aggregation may be counterproductive. Rigid systems typically have better organization, but are inherently less dynamic. This work shows that ion transport by amphiphilic heptapeptides (synthetic anion transporters or SATs) is affected by aggregation of the monomers in the bulk aqueous phase to which they are added and within the bilayer. Ion transport was assessed for all compounds by assay of Cl^- release from liposomes. The mechanism of ion transport was confirmed by planar bilayer conductance studies for two compounds at opposite ends of the efficacy scale. Dynamic light scattering, the Langmuir trough, transmission electron microscopy, ion release from liposomes, and planar bilayer conductance studies were used to assess the importance of self-assembly versus aggregation in ion transport. Generally, greater aggregation was has an adverse effect on the transport, although at least dimerization is required for amphiphilic heptapeptides to readily transport Cl^-. Anion transport in these systems was found to be sensitive to changes in the C-terminal portion of the $(Gly)_3Pro$-$(Gly)_3$ sequence. Moreover, a significant difference in transport efficacy was apparent when L-Trp was replaced by D-Trp in the same position.

Keywords: aggregation · amphiphiles · anions · peptides · synthesis · transport

Introduction

The challenge of recognizing, complexing, and transporting anions[1] such as chloride is currently a major subdiscipline in the broader field of supramolecular chemistry. The importance of binding and transport in biology is evident from the extensive work underway on chloride transporters.[2] The highly evolved natural transporters such as the ClC family of proteins[3] create ion pathways through the entire membrane, but other configurations are possible that engender chloride transport.[4,5] During recent decades, a range of synthetic transporters has been reported.[6] The design of such synthetic transporters is fraught with an inherent contradiction. Stronger binding of ions is favorable for recognition, but impedes transport. Likewise, if self-assembly is required for function, extensive aggregation may be counterproductive. In this study, we record the behavior of synthetic anion transporters (SATs) of the general form $(C_{18}H_{37})_2N$-CO-CH_2OCH_2CO-$(Gly)_3$-Pro-$(Aaa)_3$-$O(CH_2)_6CH_3$ in aqueous solution and in bilayer membranes using dynamic light scattering (DLS), the Langmuir (Langmuir–Blodgett or LB) trough, transmission electron microscopy (TEM), ion release from synthetic vesicles, and planar bilayer conductance measurements.

Most of the synthetic, pore-forming amphiphiles reported thus far were designed to be injected into the bulk aqueous phase that surrounds either a liposome or a cell. The compound must at least insert into the bilayer from the aqueous phase and, depending on the design, may be required to associate within the bilayer. To be sure, some very simple structures can form pores. The classic example is Triton X-100,[7] which showed ion transport activity in a planar bilayer conductance experiment when embedded in the bilayer during membrane formation. When added from the bulk phase, channel function by this simple detergent was not observed.[8]

Amphiphiles added to an aqueous suspension of liposomes may disperse or aggregate in water, they may partition into the bilayer, an aggregate in the bulk phase may fuse with the liposomal bilayer, the monomers may aggregate within the bilayer and aggregates may dissociate into monomers or smaller aggregates. Each of these reactions is part of the pore-formation dynamic, but relatively little systematic study has been devoted to this issue, notwithstanding our own previous study of these possibilities with respect to $R^1{}_2N$-$COCH_2OCH_2CO$-$(Aaa)_7$-OR^2 has addressed any of these issues for synthetic amphiphiles.[9]

The importance of such studies is exemplified by recent reports by Yang and co-workers[10] of an aromatic bis-

[a] M. M. Daschbach, S. Negin, L. You, G. W. Gokel
Center for Nanoscience, and
Departments of Chemistry & Biochemistry and Biology
University of Missouri—St. Louis, St. Louis, MO 6312 (USA)
E-mail: gokelg@umsl.edu

[b] M. Walsh
Department of Science and Mathematics
Maryville University, St. Louis, MO 63141 (USA)

[c] G. W. Gokel
Departments of Developmental Biology and Chemistry
Washington University, St. Louis, MO 63130 (USA)

(leucine) derivative that shows classic open–close, channel-type behavior, but is far too small to span a bilayer. A self-assembly mechanism has been reported by DeGrado and co-workers for various lysine-substituted isophthalamides that exhibit antibiotic activity.[11] To our knowledge, the mechanism of transport remains obscure or unreported in both cases and, indeed, in most systems despite the fact that self-assembly must be critical. It is certainly true that studies have been reported in which insertion dynamics have been addressed, but these did not consider aqueous solution aggregation or aggregate insertion into the bilayer. The question of monomers associating with a membrane before insertion has been considered by Matile,[12] Fyles,[13] and their co-workers in the context of pore formation and also in the context of antibiotic activity. Shai's "carpet" mechanism,[14] for example, recognizes that a two- or multistep process must occur in order to lead to membrane penetration.

In the work reported here, we have incorporated tryptophan[15] in the heptapeptide sequence. Tryptophan is the rarest of the 20 common amino acids,[16] but occurs in proteins such as the KcsA potassium channel exclusively near the membrane–aqueous interfaces.[17] Various model systems have been designed to probe the role of tryptophan as a membrane anchor,[18–20] both experimentally[21] and computationally.[22] Work in our laboratory showed that indole itself could function as an amphiphilic headgroup in the formation of vesicles.[23] We have studied the behavior of a family of amphiphilic heptapeptides by using the range of techniques noted above and found dramatic differences in aggregation behavior both in the bulk phase and the bilayer as well as significant differences in ion transport function.

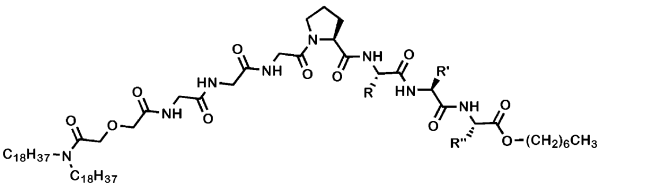

Peptide sequence in $(n\text{-}C_{18}H_{37})_2N\text{-}COCH_2OCH_2CO\text{-}Gly\text{-}Gly\text{-}Gly\text{-}Pro\text{-}(Aaa)_3\text{-}O\text{-}n\text{-}C_7H_{15}$

1, GGG	8, GWG
2, EGG	9, GGE(OBn)
3, FGG	10, GGE(pyrene)
4, WGG	11, GGK(NBD)
5, wGG	12, GGW
6, GAG	13, GGW(N-CHO)
7, GEG	14, GGW(N-CH_3)

Results

Compounds studied: Fourteen amphiphilic heptapeptides with the general formula $(n\text{-}C_{18}H_{37})_2NCOCH_2OCH_2CO\text{-}(Gly)_3\text{-}Pro\text{-}(Aaa)_3\text{-}O\text{-}n\text{-}C_7H_{15}$ were prepared for this study. These amphiphiles contain three key elements. The N-terminal, twin *n*-octadecyl chains comprise a hydrophobic membrane anchor. The C-terminal *n*-heptyl chain serves as a secondary membrane anchor as well as blunting the carboxyl group's charge. The N-terminal hydrocarbon chains are linked to the peptide through diglycolic acid as its diamide. The heptapeptide comprises the polar headgroup in which the first four amino acids are Gly-Gly-Gly-Pro. All 14 compounds are identical except for the three C-terminal amino acids. Each compound can be specified by naming these three amino acids. Thus, we refer to $(n\text{-}C_{18}H_{37})_2NCOCH_2OCH_2CO\text{-}(Gly)_3\text{-}Pro\text{-}Glu\text{-}Gly\text{-}Gly\text{-}O\text{-}n\text{-}C_7H_{15}$ (**2**) as **EGG** (for Glu-Gly-Gly).

The amphiphilic heptapeptides were synthesized by using wet chemical methods[24] as follows. Dioctadecylamine was heated in toluene with diglycolic anhydride to give $(n\text{-}C_{18}H_{37})_2NCOCH_2O\text{-}CH_2COOH$ after evaporation of the solvent. This fragment was coupled to commercial triglycine to give $(n\text{-}C_{18}H_{37})_2NCOCH_2O\text{-}CH_2CO\text{-}(Gly)_3\text{-}OH$. The peptide fragment comprising the fourth to seventh amino acids was likewise prepared by using standard conditions, esterified, and then linked to the acylated N-terminal fragment. The general structure of the compounds discussed is shown above and the sequences are identified by the amino acids in the 5–7 positions in Table 1.

Table 1. Peptide sequence in $(n\text{-}C_{18}H_{37})_2N\text{-}COCH_2OCH_2CO\text{-}(Aaa)_7\text{-}O\text{-}n\text{-}C_7H_{15}$ and percent of total Cl^- release from DOPC/DOPA (7:3) liposomes measured at 1800 s.

	Sequence	Cl [%]		Sequence	Cl [%]
1	GGGPGGG	35	**8**	GGGPGWG	40
2	GGGPEGG	15	**9**	GGGPGGE(OBn)	70
3	GGGPFGG	20	**10**	GGGPGGE(pyrene)	70
4	GGGPWGG	10	**11**	GGGPGGK(NBD)	45
5	GGGPwGG	21	**12**	GGGPGGW	25
6	GGGPGAG	50	**13**	GGGPGGW(N-CHO)	60
7	GGGPGEG	20	**14**	GGGPGGW(N-CH_3)	30

The tryptophan-containing synthetic anion transporters (**4**: **WGG**; **5**: **wGG**; **8**: **GWG**; and **12**: **GGW**) are the primary subject of this study. The syntheses of the other compounds have previously been reported (see the Experimental Section). Scheme 1 (below) provides an example for the synthetic route used to obtain **WGG**, **wGG**, **GWG**, and **GGW**.[13] Note that "w" denotes D-stereochemistry, whereas "W" denotes the more common L-isomer.

Chloride transport—different amino acid sequences and membrane compositions: Chloride transport mediated by **WGG**, **wGG**, **GWG**, and **GGW** was determined by using vesicles prepared from either 1,2-dioleoyl-*sn*-glycero-3-phosphocholine (DOPC) or from 7:3 (w/w) DOPC and 1,2-dioleoyl-*sn*-glycero-3-phosphate (DOPA, see the Experimental Section of reference [24]). Briefly, a KCl buffer was trapped within the vesicles, which were then suspended in K_2SO_4 buffer. Each compound was then added to the vesicle suspension and insertion into the bilayer and pore-formation were inferred by detecting chloride release. The emergence of Cl^- from the liposomes was recorded by using a chloride-selective electrode inserted into the vesicle suspension.[27] At the end of each trial, sufficient detergent (Triton X-100) was

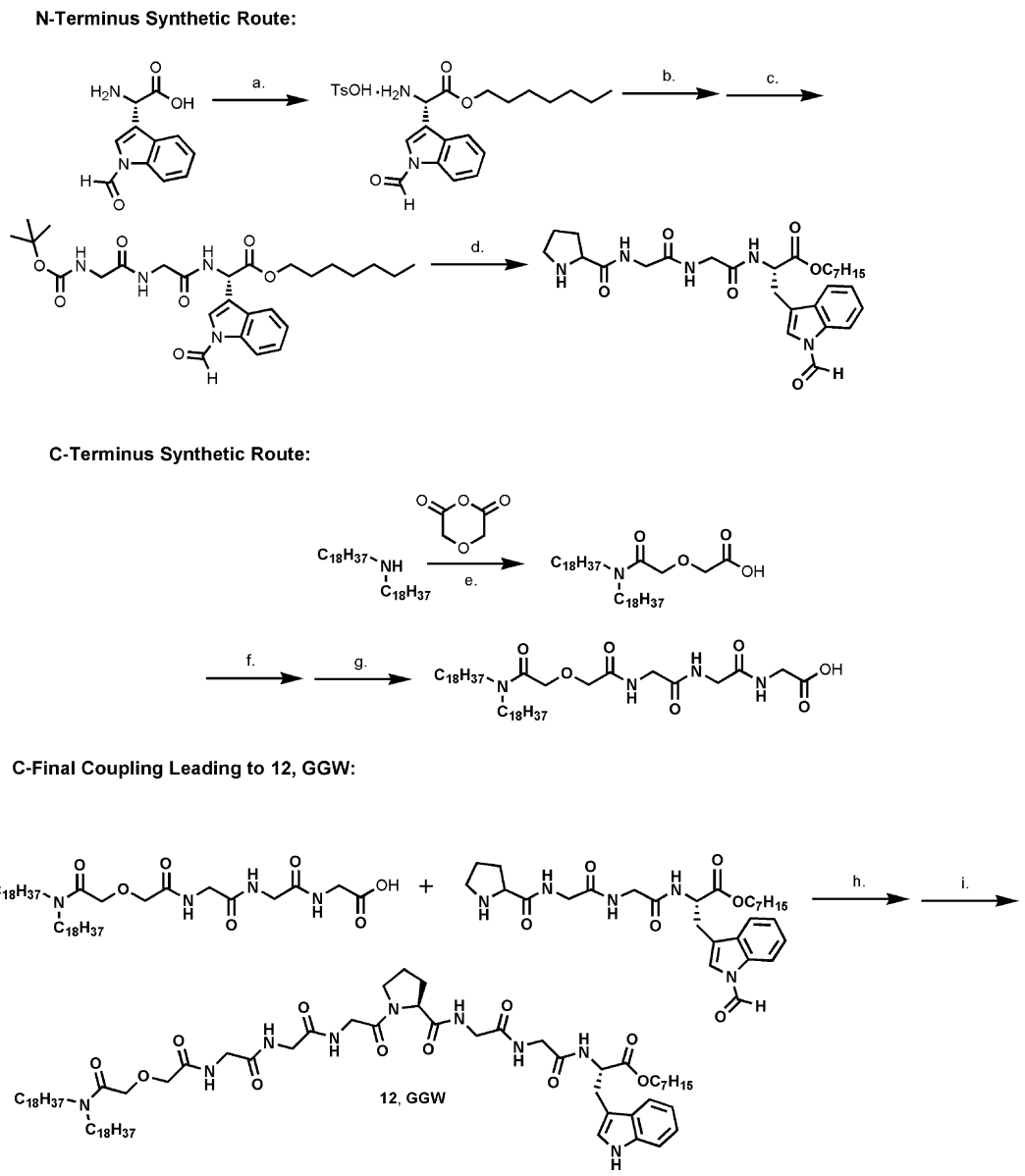

Scheme 1. Synthetic route to **12**, **GGW**. N-terminus: a) 1-heptanol, toluene, 58%; b) 1. *N*-Boc-Gly, EDCI, HOBt, NEt_3, CH_2Cl_2, 62%, 2. Boc removed with 4N HCl/dioxane; c) 1. *N*-Boc-Gly, EDCI, HOBt, NEt_3, CH_2Cl_2, 56%, 2. Boc removed with 4N HCl/dioxane; d) 1. *N*-Boc-Pro, EDCI, HOBt, NEt_3, CH_2Cl_2, 98%, 2 HCl/dioxane. C-terminus (synthesis has been described previously[25]): e) toluene, reflux, 87%; f) TsOHGly-Gly-Gly-OCH_2Ph, EDCI, HOBt, NEt_3, CH_2Cl_2, 89%; g) H_2, 10% Pd/C, ethanol, 96%. Final Coupling: h) EDCI, HOBt, NEt_3, CH_2Cl_2, 38%; i) NaOH, THF, 73%.

added to induce vesicular lysis and the total chloride concentration was determined. The release data were normalized to $[Cl^-]_{final}$. The chloride release data for **WGG**, **wGG**, **GWG**, and **GGW** are shown in Figure 1. Each data set is the average of at least three independent measurements.

Release of Cl^- from vesicles mediated by **WGG**, **wGG**, **GWG**, or **GGW**, is a well-behaved process. The 1800 s time value was chosen because ion release has often reached a plateau by that time and/or the trend in transport behavior is clear.[28] Several of the experiments were monitored to longer times, but those data sets were truncated for consistency of presentation. In no case was any anomaly observed at longer times.

The difference in the abilities of **WGG**, **wGG**, **GWG**, and **GGW** to transport Cl^- is striking. The fractional ion release values from DOPC/DOPA (7:3) liposomes for Cl^- observed at the 1800 s time point are **WGG** = 0.10, **wGG** = 0.21, **GWG** = 0.40, and **GGW** = 0.25. Thus, for these peptides, transport diminishes in the order **GWG** > **GGW** > **wGG** > **WGG**. The same general trend is observed for fractional ion release from DOPC liposomes. At 1800 s, the normalized release values are as follows: **WGG** = 0.28, **GGW** = 0.16, **WGG** = 0.11, and **wGG** = 0.08. Thus the trend in the absence of DOPA is **GWG** > **GGW** > **WGG** > **wGG**.

The percentage of chloride released from DOPC/DOPA (7:3) at 1800 s is summarized in Table 1 for compounds **1**–**14**. Each of these experiments was conducted as described

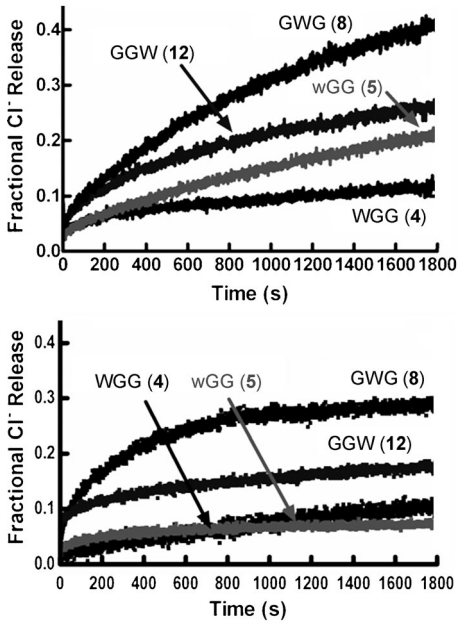

Figure 1. Chloride release from DOPC/DOPA (7:3) liposomes (0.31 mM, left panel) and DOPC liposomes (0.31 mM, right panel) mediated by **4** (**WGG**), **5** (**wGG**), **8** (**GWG**), and **12** (**GGW**) (65 μM at pH 7). No Cl^- leakage above baseline was observed in the absence of a transporter.

above for **WGG**, **wGG**, **GWG**, and **GGW**. The indoyl side chain of tryptophan can form hydrogen bonds, cation–π contacts, and it adds steric bulk to the SAT. To be sure that the effect of tryptophan substitution is unique to tryptophan and not to any one of the aforementioned properties, we have included substitutions that can form electrostatic contacts, have different electron-rich π systems, and add steric bulk. There is no evident trend. Steric bulk, such as that in **3** (**FGG**) decreased transport efficacy while that in **10** (**GGE-(pyrene)**) and **11** (**GGK(NBD)**) increased transport efficacy. Disallowing indoyl hydrogen bonding through acylation (**13**, **GGW(N-CHO)**) and alkylation (**14**, **GGW(N-CH_3)**) increased and decreased the SAT's ability to transport Cl^-, respectively. Finally, the identity of the π system (**3**, **FGG**), the electron density of the π system (**13**, **GGW(N-CHO)** and **14**, **GGW(N-CH_3)**), and the stereochemistry of the tryptophan side chain (**4**, **WGG** and **5**, **wGG**) all had varying effects on anion transport.

Planar bilayer studies: Release of Cl^- from liposomes may occur either by a carrier mechanism or by pore formation. These mechanisms may be distinguished by using the planar bilayer voltage clamp conductance technique. The experiment uses two chambers (cuvettes) connected by a hole of approximately 200 μm. When a bilayer forms in the orifice, solutions in the two chambers are insulated from one another. Addition of a pore-former allows ions present in one chamber to pass through the membrane and to carry current, which is detected at a specific voltage (voltage clamp) as a function of time. No current is detected when the pore is closed. The observation of open–close behavior confirms pore formation. The studies reported here used asolectin membranes and the buffers contained 450 mM KCl and 10 mM HEPES at pH 7. Each ionophore was dissolved in 2,2,2-trifluoroethanol (TFE). The solution was added to the cis-chamber resulting in a compound concentration of 2 μM.

Fyles[13] has pointed out that "[v]esicle techniques offer more scope for structure–activity surveys, and there are many examples of this type of investigation. Even so, vesicle techniques are subject to artefacts as the hoped-for channel activity is often indistinguishable from the detergent-like lysis of the vesicles." In the present study, the parent peptide, **GGGPGGG**, and variants **WGG**, and **wGG** were examined by the planar bilayer conductance method. The last two compounds are the poorest transporters among the tryptophan-containing peptides. The channel-forming properties of **GGG** are well documented.[26] Our assumption was that if a good transporter (**GGG**) and the poorest Trp-containing compounds (**WGG**, **wGG**) showed ion-channel behavior, it was reasonable to assume that the range of compounds shown in Table 1 all formed conducting pores. In addition, previous studies of **GGE** (not shown in Table 1) in DOPC/DOPA bilayers showed channel activity and a conductance of about 30 picoSiemens (pS).[27] All three peptides, **GGG**, **WGG**, and **wGG**, showed well-defined open–close behavior at applied potentials between 20 and 50 mV (see Figure 2).

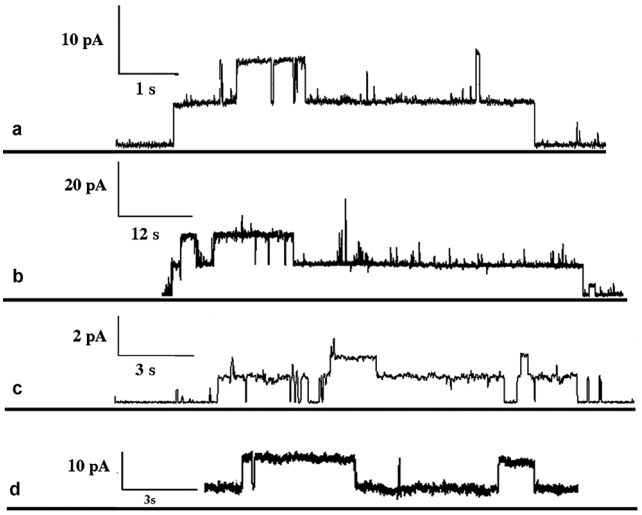

Figure 2. Single-channel traces for a) **GGG** (**1**), 20 mV; b) **GGG** (**1**), 40 mV; c) **WGG** (**12**), 50 mV; d) **wGG** (**5**), 50 mV.

Figure 2 shows planar bilayer conductance data obtained in asolectin membranes for **GGG** (panels a and b), **WGG** (panel c), and **wGG** (panel d). The traces for **GGG** were obtained at 20 and 40 mV and their conductances (ca. 6.5 and 11 pA) correspond. The results for **WGG** and **wGG** were significantly different from those obtained for **GGG** and from each other. The current for **WGG** was about 1.2 pA and for **wGG** it was nearly sixfold greater (i.e., ca. 8 pA), each at 50 mV. When the three amphiphilic peptides were compared, they showed the trend **GGG** > **wGG** > **WGG**, re-

gardless of whether transport was measured by ion release from liposomes or by planar bilayer conductance measurements.

Dynamic light scattering and transmission electron microscopy: In the experiments described herein, the ionophore is added as a solution in an appropriate solvent to the aqueous phase that bathes the membrane. When a solution containing the ionophore is added to the aqueous buffer, it is likely that the amphiphiles aggregate as occurs in the formation of micelles. The formation of aggregates in aqueous suspension can be detected by dynamic light scattering (DLS). The DLS method uses the scattering of a laser beam that passes through a solvent (water in all cases described here) to detect and determine the size of the aggregates formed in the suspension. Compounds **GGG** (control), **WGG**, **wGG**, **GWG**, and **GGW** were suspended in water (30 μM) in an effort to detect aggregates. No aggregation was apparent for **GGG** at any concentration studied (5–100 μM); at concentrations >100 μM, **GGG** precipitated from water. Similar treatment of **GWG** gave data that suggested aggregation, but the experiments were not reproducible. We infer that while **GWG** does self-assemble in aqueous suspension, a range of aggregates forms: the DLS instrument reported different polydispersities in separate experiments conducted at identical concentrations. Thus, nine trials yielded average smaller and larger diameters of (50±6) and (155±53) nm, respectively.

DLS showed stable, bimodal distributions for **WGG**, **wGG**, and **GGW**. All three compounds formed aggregates about 50 nm (ca. 500 Å) in diameter. The larger aggregates showed hydrodynamic diameters of approximately 150, 160, and 120 nm, respectively. The aggregate distributions for **WGG**, **wGG**, and **GGW** were reproducible [averages (9 trials), **WGG**: (56±4), (151±8) nm; **wGG:** (54±6), (163±11) nm; **GGW**: (53±3), (116±9) nm] and stable for >24 h [$(\mathbf{WGG})_n$ was stable for >72 h]. We note that **GGG** and **GWG** are superior as Cl^- transporters to **WGG**, **wGG**, and **GGW**. Thus, poor anion transport appears to correlate with stable aggregate formation (**WGG**, **wGG**, or **GGW**). We were unable to detect stable aggregate formation for good Cl^- transporters **GGG** and **GWG**.

The formidable DLS method gives no structural information. Transmission electron micrographs (TEMs) were therefore obtained for any samples that were stable enough to be studied by this method. Samples were prepared by evaporation and deposition onto carbon-coated copper grids. We previously observed bimodal distributions for related ionophores that had C-terminal benzyl rather than *n*-heptyl esters only by DLS, but could not confirm them by microscopy.[30]

The right panel of TEM Figure 3 shows spherical aggregates (ca. 30–70 nm) of **WGG** that correspond to the smaller size in the bimodal distribution. TEM images were obtained when a single glycine replaced L-tryptophan in the fifth position of the heptapeptide sequence (**GGG**→**WGG**), but no image could be obtained for **GGG**. The left panel of

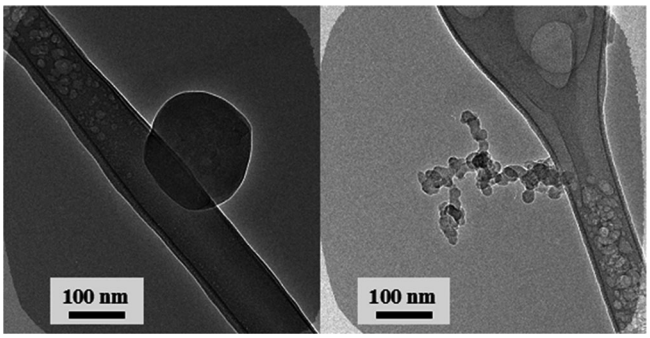

Figure 3. Transmission electron micrographs of aggregates comprised of compound **4**, $(C_{18}H_{37})_2NCOCH_2OCH_2CO$-GGGP**WGG**-$OC_7H_{15}$, on a copper grid. Left panel: 200 nm single structure. Right panel: 30-70 nm distribution.

Figure 3 shows an aggregate larger than recorded by DLS, but the latter is a statistical average. The structure shown could be at the outer edge of the distribution or it could have undergone a "pancake" effect during sample preparation. In either event, it is important to note that **WGG**, **wGG**, and **GGW** form aggregates that can be detected by more than one analytical technique and the more active transporter amphiphiles **GGG** and **GWG** do not.

Langmuir trough isotherm data: The Langmuir trough provides a means to assess the dynamic organization of amphiphiles at the air–water interface. The Langmuir trough consists of a "pan of water" and two lateral barriers that can be moved towards each other to reduce the available surface area. An amphiphile is spread on the aqueous surface, the barriers are moved to compress the monolayer, and the resulting forces are reported by a transducer called a Wilhelmy plate. The data obtained give information about the organization of the amphiphile, its minimum size requirements, and the overall stability of the system.

We previously reported reproducible phase transitions at (176±6) and (68±4) nm for **GGG**.[30] Similar studies were conducted as part of this work with **WGG**, **wGG**, **GWG**, and **GGW**. The trough experiments were replicated as many as 12 times for each amphiphile in a failed effort to achieve reproducibility. Although generally similar behavior was observed for each compound in the various runs, significant enough differences were observed in enough replicates to preclude a valid discussion of the data. Since our principal interest concerning the function of the SATs was their behavior in the presence of phospholipids, the amphiphiles were co-spread with either 1,2-dioleoyl-*sn*-glycero-3-phosphocholine (DOPC) or 1,2-dioleoyl-*sn*-glycero-3-phosphate (DOPA), the same lipids used for the Cl^- release studies (*see* above).

Compounds **WGG**, **wGG**, **GWG**, and **GGW** and the phospholipid DOPC were co-spread (1:1 mol:mol DOPC/SAT) on the aqueous phase of a Langmuir trough. Compounds **WGG**, **wGG**, **GWG**, and **GGW** were also co-spread with the phospholipids DOPC and DOPA (7:3:10 mol:mol:mol

DOPC/DOPA/SAT). The trough barriers were moved from a surface area of about 200 Å^2 at a rate of approximately 20 Å^2 molecule^{-1} min^{-1} until collapse was observed. The resulting isotherms are shown in Figure 4.

The presence of DOPA (plus DOPC) appears not to affect monolayer formation when mixed with **WGG**; the two isotherms are essentially superimposable (Figure 4, top panel). The monolayer formed from DOPA/DOPC and **GGW** differs modestly from that formed from **GGW** and DOPC alone. In the presence of DOPA (and DOPC), a shift to smaller molecular areas are observed for **GGW**. This suggests a closer molecular packing in the mixture. The most pronounced shift occurs when GWG is co-spread with DOPA: the monolayer's transition point and collapse are approximately 50 and 20 Å^2 smaller, respectively. Figure 4 also reveals an interesting stereochemical effect for the isomers **WGG** and **wGG**. The isotherms for the D-isomer, **wGG**, show smaller molecular areas in the presence of DOPA than when **WGG** is present with DOPC/DOPA. In the absence of DOPA, **wGG** and **WGG** show very similar results. This is discussed in a later section.

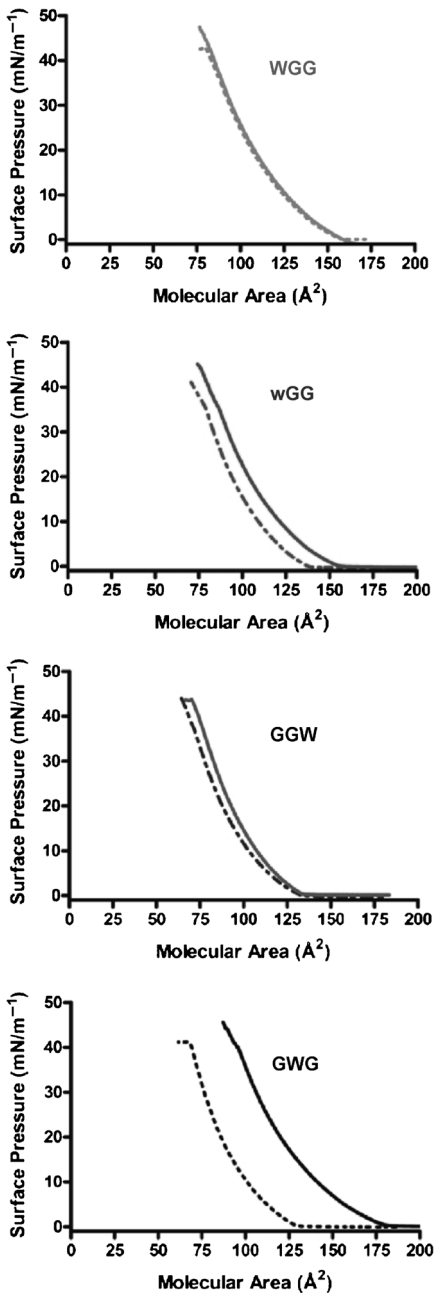

Figure 4. Surface pressure-area (π–A) isotherm data for co-spread monolayers, DOPC:$(C_{18}H_{37})_2NCOCH_2OCH_2CO$-$(Gly)_3$-Pro-$(Aaa)_3$-$OC_7H_{15}$ (1:1, mol:mol), solid lines. Transitions: **WGG** (**4**) and DOPC: 152, 80 Å. **GGW** (**12**) and DOPC: 133, 71 Å^2. **wGG** (**5**) and DOPC: 152, 75 Å^2. **GWG** (**8**) and DOPC: 180, 90 Å^2. DOPC/DOPA:$(C_{18}H_{37})_2$-$NCOCH_2OCH_2CO$-$(Gly)_3$-Pro-$(Aaa)_3$-OC_7H_{15}. (7:3:10, mol:mol:mol), dashed lines. Transitions: **WGG** (**4**) and DOPC/DOPA: 154, 76 Å^2. **wGG** (**5**) and DOPC/DOPA: 138, 71 Å^2. **GWG** (**8**) and DOPC/DOPA: 130, 68 Å^2. **GGW** (**12**) and DOPC/DOPA: 132, 62 Å^2.

Discussion

Chemical equilibria involved in pore formation: In principle, the formation of a conducting pore in a bilayer must involve several steps. When the ionophore is added to an aqueous suspension of vesicles, it can disperse, aggregate, or associate with the external membrane of the liposome. If aggregates form, the ability of amphiphile monomers to associate with the liposomes will be reduced and the formation of pores will ultimately be slowed. Once the ionophores associate with the liposomes, they must insert in the bilayer. Aggregation may occur within the bilayer that does not involve pore formation. Individual monomers can diffuse laterally within the membrane, ultimately organizing into a conducting pore.

Each of these processes will have a rate specific to the compound and medium. The combination of rates will determine how effectively, if at all, a pore forms. In addition, the transport rate may be affected by the presence of a charge within the conducting pore, as we have observed when a glutamic acid residue is present in the heptapeptide.[13] Scheme 2 shows the minimum equilibria involved in pore formation within a vesicular membrane when an amphiphilic ionophore is added to an aqueous liposome suspension. Ideally, k_1, k_3, k_4, and k_5 would all be large and the reverse rates would all be small. The formation of inactive aggregates will be favored by larger values of k_2 and k_6.

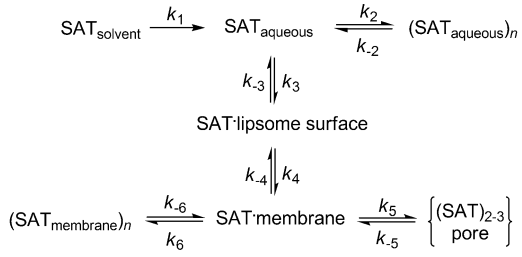

Scheme 2. Chemical equilibria involved in SAT pore formation.

Dynamic light scattering and transmission electron microscopy: We have recently reported the use of various fluorescent probes to examine the behavior of SATs in aqueous solution and in the phospholipid bilayer. The key findings of those studies were as follows. First, SATs aggregate in the bulk aqueous phase. The observation of pyrene excimer formation demonstrated this for an appropriately substituted SAT amphiphile/ionophore. Both monomer and excimer emission were observed when these derivatives were inserted in liposomes. The fluorescent dye NBD (4-fluoro-7-nitrobenz-2-oxa-1,3-diazole) is quenched in water, but less in hydrocarbon media. Using this difference in behavior, we determined that about 35% of an NBD-substituted SAT partitioned into the bilayer.[15] Formation of aggregated pores was confirmed by fluorescence resonance energy transfer from a tryptophan-substituted SAT to a pyrenyl-SAT.

The goal of the present study was to understand the dynamics of self-assembly and to assess whether aggregation, either in the bilayer or the bulk aqueous phase, correlated to transport. In all of our studies, we add the ionophore to a membrane-containing phase rather than pre-mixing it. This is done to preclude the type of behavior observed for Triton X-100 described in the Introduction. The dynamic light scattering technique was used in the expectation that aggregation behavior and transport efficacy could be correlated. As noted above, **GGG** is one of the more active Cl^- transporters studied. No aggregates could be detected in aqueous suspension at any concentration between 10–100 μM. At higher concentrations, the compound precipitated from solution. These experiments suggest an inverse relationship between aqueous phase aggregation and bilayer transport.

A number of SAT derivatives not included in the present studies showed bimodal distributions by DLS, but only the larger aggregates could be detected by TEM. When any of the three C-terminal glycine residues (positions 5, 6, or 7) was replaced by tryptophan, aggregation was observed (DLS). Poor Cl^- transporters **WGG**, **wGG**, and **GGW** showed similar bimodal distributions when suspended in water. In all cases, the aggregates were calculated by the instrument's internal software to be about 150 nm and about 50 nm in diameter. In the case of **GGW** and **WGG**, both DLS and TEM confirm the presence of large and small assemblies. The DLS software assumes spherical aggregates, a credible assumption based on the TEM results shown above (Figure 3).

Tryptophan-containing SAT **GWG** shows Cl^- transport behavior (40% release) approximately equal to that of **GGG** (35%) and superior to **WGG** (10%), **wGG** (21%), or **GGW** (25%). DLS experiments indicated that **GWG** formed aggregates in water. Unfortunately, neither size nor polydispersity of these aggregates proved to be reproducible in more than ten experiments. This behavior contrasts with the aggregates formed from **GGW**, **WGG**, or **wGG**, which formed well-defined aggregates that were stable in suspension for many hours.

Within the group of compounds **GGG**, **WGG**, **wGG**, **GWG**, and **GGW**, it appears that the ability to form and to observe aggregates in aqueous suspension is inversely correlated to Cl^- transport efficacy. This is true whether tryptophan at position 5 has L- (**WGG**) or D-stereochemistry (**wGG**). We note that Cl^- transport by the latter is significantly better than its stereoisomer (see further discussion below).

Planar bilayer conductance: The traces shown in Figure 2 (above) clearly show classic open–close behavior for **GGG**, **WGG**, and **wGG**. The observed conductance for **GGG** (35% Cl^- release) is 257 picoSiemens (pS) compared to 28 pS for **WGG** (10% Cl^- release). Using Hille's equation to estimate pore size from conductance values,[31] the pore diameters of **GGG** and **WGG** are about 10 and 4 Å, respectively. We have previously reported an estimated pore size for **GGG** of approximately 8–9 Å based on computational and physical models and on the synthesis of pseudodimers.[32] A solvated Cl^- ion is estimated to be a sphere of about 6.5 Å in diameter.[33] The estimated pore size of approximately 4 Å for **WGG** suggests that either it functions as a monomer or that the dimer, if formed, is far more compressed than for **GGG**. A smaller or more rigid pore would certainly show poorer ion transport and this comports with the poorer Cl^- release measured for **WGG** in liposomal bilayers. Figure 2 also shows a significant difference in the behavior of **WGG** and **wGG**. The principal conductance state of **wGG** is about sixfold larger than **WGG**. Since these two molecules are isomers, the variance in conductance must result from the difference in stereochemistry, that is, the orientation of indolylmethyl group with respect to the main peptide chain. In the liposomal studies, this difference is only twofold, but it is in the same direction.

The kinetics of pore formation is also different for **GGG** and **WGG** as judged from ion release experiments. Pore formation and ion conductance are both observed first for **WGG** rather than for **GGG**. However, **GGG** forms pores that are larger and exhibit nearly tenfold greater conductance. The DLS data (see above) suggest that **GGG** does not aggregate in an aqueous suspension, but **WGG** does. We interpret this to mean that **WGG** aggregates contact the liposomal surface and penetrate the bilayer as an aggregate. Partial dissociation of monomers gives a conducting pore. In contrast, the non-aggregated **GGG** monomers likely insert individually into the bilayer and must then diffuse within the membrane and organize into a pore. Since the pore formed from **GGG** is larger than that formed from **WGG**, it must require at least two monomers. Thus, ion currents are observed for **GGG** more slowly than for **WGG**, but the conductances are higher for the former once ions flow.

It is important to note that the higher conductance observed by planar bilayer measurements for **GGG** than for **WGG** corresponds to the vesicle-release data. This is so even though ion release from vesicles is generally thought to reflect insertion dynamics rather than the formation of an

Table 2. Effect of lipid composition on monolayer formation and comparison with Cl^- transport rates.

	Cl^- release [%][a]	Molecular areas [Å^2] SAT + DOPC + DOPA		Cl^- release [%][b]	Molecular area [Å^2] SAT + DOPC		Change in Cl^- release [%]	Molecular area [Å^2] average change
WGG	10	154	76	10	152	80	0	1
wGG	21	138	71	10	152	75	11	9
GWG	40	130	68	28	180	90	12	35
GGW	20	131	62	16	133	71	4	5

[a] Cl^- release from DOPC/ DOPA (7:3) vesicles. [b] Cl^- release from DOPC vesicles.

ideal pore. The present study shows that the dynamic is more complex.

Langmuir trough studies of tryptophan-containing SATs: Figure 4 shows the monolayer behavior of WGG, wGG, GWG, and GGW in the presence of DOPC and DOPC/ DOPA; the molar ratios of which were 1:1 (SAT/DOPC) and 10:7:3 (SAT/DOPC/DOPA). For the DOPC/DOPA systems, the phospholipid monomers are in the same ratio used in the vesicle release experiments and in essentially all previous studies of these compounds. A molar equivalent of SAT was added so that any organizational effect would be apparent. In the vesicle experiments, the ratio of SAT to phospholipids is lower (see Experimental Section). It is important to note that the reproducibility of the Langmuir trough data is high. Each trace shown herein results from a minimum of 9 and as many as 12 replicates. A difference of 10% in a transition area or collapse pressure is significant. Table 2 presents comparative data for Cl^- release from vesicles and the behavior observed when studied on the Langmuir trough.

The second column of Table 2 summarizes the ion release (as a percent, observed at 1800 s) from DOPC/DOPA (7:3) vesicles. The order of transport efficacy is **WGG** < **wGG** ≈ **GGW** < **GWG**. When the liposomes are comprised of DOPC only, Cl^- transport is diminished overall, but the efficacy order remains similar: **WGG** ≈ **wGG** < **GGW** < **GWG**. Table 2 also records the difference in percentage Cl^- release from liposomes and the average change in molecular area. This gives a number that does not have independent physical meaning, but reflects organization in the monolayer and can be correlated to the differences in transport values.

The presence of tryptophan in position 5, 6, or 7 of the heptapeptide sequence clearly affects the interactions between the SAT and the surrounding phospholipids. The monolayer behavior of **WGG** is the same in DOPC or in DOPC/DOPA. The molecular areas of **wGG**, **GWG**, and **GGW** are all shifted to smaller values in the presence of DOPA. The magnitude of the change increases in the order **GGW** < **wGG** < **GWG**. Chloride ion transport is also affected by the presence of DOPA, except for **WGG** (ca. 10% in either lipid). For **GGW**, **wGG**, and **GWG**, fractional release at 1800 s decreases in the absence of DOPA. The magnitude of this change increases in the order **GGW** < **wGG** < **GWG**. These data, like the aggregation data, suggest that molecular organization and transport efficacy are correlated. Of course, inversion of the stereochemistry in **wGG** compared to **WGG** means that the amino acid lies on opposite sides of the main chain.

The effects of tryptophan: The presence of tryptophan may alter the system in at least three different ways. First, tryptophan is regarded as a "membrane-anchoring group." For example, the only tryptophan residues that occur in the KcsA potassium selective channel protein occur at the membrane boundaries.[34] Even the simple dimeric gramicidin channel[35] appears to be anchored by tryptophans that occur only at its proximal and distal boundaries.[36] Other evidence includes the formation of stable vesicles from monoalkyl-substituted indoles.[37]

Second, tryptophan's indole residue has been extensively studied as a donor in cation–π interactions that involve metallic and ammonium cations. Evidence for the latter emerged a quarter century ago in the pioneering study of peptide interactions reported by Burley and Petsko.[38] Dougherty and co-workers have demonstrated that cation–π interactions involving Na^+ or K^+ can play a critical role in channel function.[39] Third, we have shown that synthetic ion transporters show varying efficacies when cation–π interactions between DOPC and aromatic side chains can occur.[40] These effects are not observed when DOPC is mixed with DOPA, which helps to neutralize the former's ammonium headgroup charge.

Postulated interaction between SAT and DOPA: It is well established from our earlier work that the SAT amphiphiles complex and transport Cl^- ions through the bilayer. An NMR structure for a GGGPGGG peptide in the presence of $Bu_4N^+Cl^-$ was obtained in collaboration with Tomich and co-workers.[41] The structure showed that Cl^- was bound by the amide hydrogens of glycines 5 and 7. In principle, the same general type of assembly may form on the Langmuir trough in which an oxygen atom of DOPA acts as the anion and the DOPC headgroup is positioned as is Bu_4N^+ in the known complex. This possibility is illustrated in Figure 5, both schematically and with space-filling models. Compound **wGG** is positioned so that the DOPA headgroup resides in the cavity known to interact with Cl^- in the published study.[40]

As noted above (Figure 4), there is no difference in the isotherms observed for **WGG** and DOPC in the presence or absence of DOPA. This might seem unreasonable considering that DOPA is negatively charged and DOPC is neutral (zwitterionic). Figure 6 shows an end view of diacetylphos-

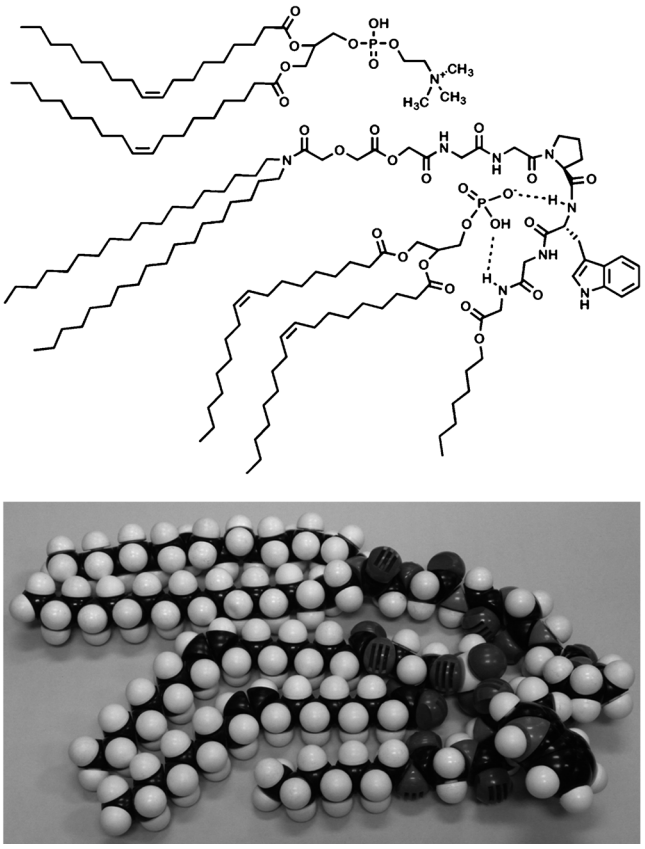

Figure 5. Schematic and space-filling molecular model representations of postulated DOPA-SAT interactions.

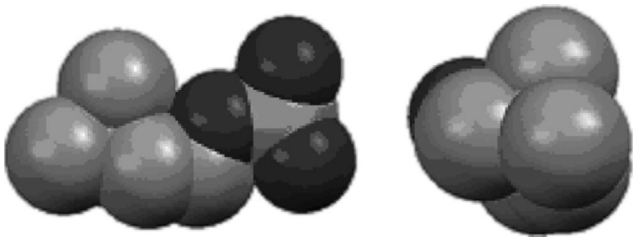

Figure 6. Calculated space-filling molecular models showing the headgroups (side and end views) of diacetylphosphatidylcholine (hydrogen atoms omitted).

phatidylcholine. It is apparent that the three methyl groups of choline essentially eclipse the phosphoryl oxygen atoms. Thus, the size of choline or phosphate, when either is the lipid's terminal residue, is similar. Molecular models suggest that either DOPA or DOPC can reside in the SAT's cleft, as illustrated for DOPA in Figure 5. The complexation interaction is expected to be enhanced for DOPA by electrostatics, although the extent of the increase is hard to judge considering the multiplicity of weak forces that can act in this system.

The space-filling representation in Figure 5 shows that tryptophan protrudes from the peptide chain and the direction of that protrusion is dependent on the amino acid's stereochemistry. If a side chain is present at position 5 or 7, the residue will be on one side of the extended molecule and on the other when in position 6. Looking down on the structure fragment shown in Scheme 3, positions 5 and 7 place the side chains "upward" and position 6 faces "downward." Reversing the stereochemistry from L to D in any position inverts this placement.

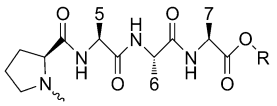

Scheme 3. C-terminal peptide sequence.

Stereochemistry, and thus chain orientation, may permit or disallow the supramolecular interactions necessary for the Trp moiety to function as an anchor or a cation–π donor. Calculations and CPK molecular models (not shown) suggest that the tryptophan is more exposed in **wGG** and **GWG** than their isomers **WGG** and **GGW** when DOPA is bound in the SAT's cleft. Thus, the indole side chains of **wGG** and **GWG** could engage in more supramolecular contacts. A favorable cation–π contact with a DOPC headgroup, while DOPA is bound in the SAT cleft, for example, could account for the tighter packing at the air–water interface in **wGG** and **GWG** (i.e., the shift to smaller molecular areas in the SAT/DOPC/DOPA co-spread systems, see Figure 4, above). The presumption that DOPA is organizing the SAT and changing how the indole side chain is exposed is also supported by the data shown in Figure 7.

We prepared **wGG**, to assess if only the stereochemistry of tryptophan (in **WGG**) could affect transport. The difference between **wGG** and **WGG** was confirmed in studies involving ion release from vesicles (Table 2). We co-spread **wGG** and **WGG** with DOPC alone and separately with a mixture of DOPC/DOPA in a molar ratio of 7:3. No difference was observed in the monolayer behavior of **WGG** in the presence of one or both lipids. The behavior of **wGG** was significantly different: the molecular areas were an average of 11 $Å^2$ larger when **wGG** was in the presence of DOPC/DOPA compared to when DOPA was absent. These differences are apparent in the data shown in Figure 4 (above). Interestingly, in the absence of DOPA, the isotherms of **wGG** and **WGG** are essentially superimposed (Figure 7).

These data indicate that when DOPA is absent, and there is no presumed preorganization of the SAT cleft, the tryptophan would be equally exposed in the **wGG** and **WGG** systems. This presumably causes the monolayer packing to be the same for either isomer. Indeed, this is confirmed by the superimposed isotherm data sets for **wGG** and **WGG** in the absence of DOPA shown in Figure 7.

Additional confirmation can be found in the planar bilayer conductance results. In previous studies, the pores formed from SATs were typically, approximately dimeric.[32] If we assume that is the case here, then differences in conductance must relate to either the organization of the pore or to inter-

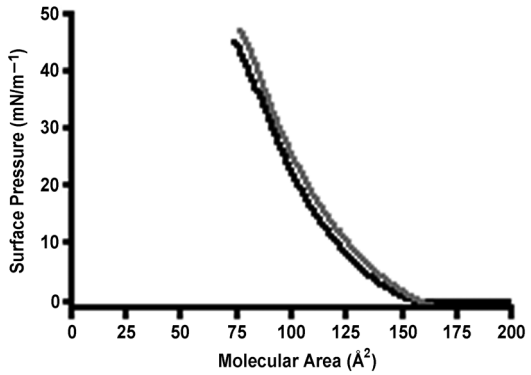

Figure 7. Surface pressure-area (π–A) isotherm data for co-spread monolayers, DOPC:$(C_{18}H_{37})_2NCOCH_2OCH_2CO$-$(Gly)_3$-Pro-$(Aaa)_3$-$OC_7H_{15}$ (1:1, mol:mol). Grey trace: **WGG** (**4**) and DOPC, Transitions: 152, 80 Å^2. Black trace: **wGG** (**5**) and DOPC, Transitions: 152, 75 Å^2.

nal hindrance. In a study of **GGE**,[29] we found that the presence of ionizable glutamate within the pore decreased ion transport. This was ascribed to the negative charge impeding Cl^- transport within the dimeric pore. In the present case, tryptophan may play one of two evident roles. On the one hand, it may turn outward from the pore and interact with positive lipid headgroups in a cation–π fashion. This could give a higher level of organization to the pore and enhance transport. Alternately, it may infiltrate the pore and reduce transport simply by steric hindrance.

Three different types of information are available with respect to this issue. First, we have measured ion release, which reflects insertion and pore-formation dynamics. Second, we have measured planar bilayer conductance, which reflects the effectiveness of transport within a pore. Third, we have information from the Langmuir trough concerning organization of the peptides both in the absence and presence of lipids. Chloride ion release from liposomes is mediated more effectively by **wGG** than by **WGG** (see Table 1). Planar bilayer conductance shows that **wGG** is a better pore-forming transporter than is **WGG** (Figure 2). Figure 4 shows that **wGG**, but not **WGG**, is sensitive to the presence of DOPA, suggesting a higher level of organization within the bilayer. In the absence of DOPA, D-tryptophan impedes the transport pathway less than does L-Trp. We conclude that the steric position of tryptophan, dictated by the two possible stereochemical arrangements, is critical to interactions with the anionic headgroups of DOPA monomers, which leads to a more organized conductance state.

Conclusion

The work presented here addresses the relationship of self-assembly and aggregation to the efficacy of Cl^- transport. A range of compounds was prepared and their ability to transport Cl^- through liposomal membranes was confirmed. Transporters at opposite ends of the efficacy scale were tested by the planar bilayer conductance method and both were shown to form pores. Aggregation in aqueous suspension was assayed by dynamic light scattering. The proclivity to aggregate in suspension was correlated to ion release from liposomes. Aggregation was further confirmed by transmission electron microscopy. The general conclusion from these studies was that those compounds that self-aggregated were generally poor ion transporters.

Tryptophan (Trp, W) was introduced as a replacement for glycine on the *C*-terminal side of proline in the heptapeptide sequence GGGPGGG. The presence of W in positions 5 or 7 gave poorer Cl^- transport activity than when the triglycine sequence was unperturbed. Good Cl^- transport was observed when W was present at position 6. Differences in Cl^- transport were also observed for the replacement of L-Trp with D-Trp in position 5. This was attributed to differences in steric interactions resulting from the side chain orientation in a presumed linear (sheet) conformation. Analyses using the Langmuir trough confirmed that better organization (closer packing) in the monolayer correlated to poorer ion transport. Differences in membrane composition (DOPC vs. DOPC/DOPA) suggested that the SAT molecules can interact with and bind the phosphoryl headgroup of DOPA, thus affecting molecular organization and pore formation.

Experimental Section

General: ^{1}H NMR (300 MHz) and ^{13}C NMR (125 MHz) spectra were recorded in $CDCl_3$ unless otherwise specified and are reported as follows: chemical shifts reported in ppm (δ) downfield from internal $(CH_3)_4Si$ (integrated intensity, multiplicity (br = broad, s = singlet, d = doublet, t = triplet, q = quartet, brs = broad singlet, m = multiplet, etc.), coupling constants in Hz, assignment. ^{13}C NMR spectra are referenced to $CDCl_3$ (77.23 ppm). Infrared spectra were recorded on a Perkin–Elmer 1710 Fourier transform infrared spectrometer. Melting points were determined on a Thomas Hoover apparatus in open capillaries and are uncorrected. Thin-layer chromatography was performed on silica gel 60-F-254 with a 0.2 mm thickness. Preparative chromatography columns were packed with silica gel (Merck grade **9385**, 230–400 mesh, 60 Å). Reagents were of the best grade commercially available and were distilled, recrystallized, or used without further purification, as appropriate. CH_2Cl_2 was distilled from calcium hydride. Reactions were conducted under N_2 unless otherwise noted. The following abbreviations are used throughout: EDCI: 1-(3-dimethylaminopropyl)-3-ethyl carbodiimide hydrochloride; HOBt: 1-hydroxybenzotriazole; TsOH: toluenesulfonic acid; DGA represents diglycoyl, $-COCH_2OCH_2CO-$. Combustion analyses were performed by M-HW Laboratories, Phoenix, AZ, and are reported as percentages.

Compound 1: $(C_{18}H_{37})_2NCOCH_2OCH_2CO$-Gly-Gly-Gly-Pro-Gly-Gly-Gly-OC_7H_{15} (**1**) was prepared as previously reported.[24]

Compound 2: $(C_{18}H_{37})_2NCOCH_2OCH_2CO$-Gly-Gly-Gly-Pro-Glu-Gly-Gly-OC_7H_{15} (**2**) was prepared as previously reported.[29]

Compound 3

$(C_{18}H_{37})_2NCOCH_2OCH_2CO$-Gly-Gly-Gly-Pro-$OCH_2Ph$: L-Proline benzyl ester·HCl (0.47 g, 1.93 mmol) was dissolved in dry CH_2Cl_2 and cooled to 0 °C. $(C_{18}H_{37})_2NCOCH_2OCH_2CO$-Gly-Gly-Gly-OH (1.56 g, 1.93 mmol, synthesis see reference [24]), EDCI (0.41 g, 2.12 mmol, 1.1 equivalents), HOBt (0.29 g, 2.12 mmol, 1.1 equiv), and NEt_3 (0.59 g, 5.79 mmol, 3 equiv, dropwise) were added successively to this solution. The reaction was stirred at 0 °C for 30 min under N_2, warmed to RT and stirred for 48 h. The solvent was evaporated in vacuo and the resulting yellow oil

was subjected to chromatography (silica gel, 95:5 CH_2Cl_2/MeOH) to afford a white solid (1.82 g, 95%). M.p. 54–56°C; ^{1}H NMR: δ=0.87 (t, J=6.9 Hz, 6H; CH_2CH_3), 1.31 (brs, 60H; $NCH_2CH_2(CH_2)_{15}CH_3$), 1.49 (brs, 4H; $NCH_2CH_2(CH_2)_{15}CH_3$), 1.98–2.01 (m, 4H; Pro $NCH_2CH_2CH_2$), 3.04 (t, J=8.1 Hz, 2H; $NCH_2CH_2(CH_2)_{15}CH_3$), 3.25 (t, J=8.1 Hz, 2H; $NCH_2CH_2(CH_2)_{15}CH_3$), 3.49–3.61 (m, 2H; Pro $NCH_2CH_2CH_2$), 3.93–4.13 (m, 7H; Gly CH_2, Pro CH), 4.27 (s, 2H; $COCH_2O$), 5.14 (s, 2H; $OCH_2C_6H_5$) 7.09 (t, J=4.5 Hz, 1H; NH), 7.28–7.38 (m, 5H; $CH_2C_6H_5$), 7.75 (t, J=5.7 Hz, 1H; NH), 8.31 ppm (t, J=6.1 Hz, 1H; NH); ^{13}C NMR ($CDCl_3$): δ=14.3, 22.9, 24.8, 27.1, 27.2, 27.8, 29.0, 29.1, 29.5, 29.5, 29.6, 29.7, 29.8, 29.9, 31.5, 32.1, 42.0, 43.0, 46.2, 46.6, 47.0, 59.0, 59.3, 67.1, 67.8, 69.8, 72.0, 123.3, 128.5, 128.8, 128.9, 135.7, 167.2, 167.5, 168.7, 169.3, 170.0, 171.1, 171.8 ppm.

$(C_{18}H_{37})_2NCOCH_2OCH_2CO$-Gly-Gly-Gly-Pro-OH: $(C_{18}H_{37})_2NCOCH_2OCH_2CO$-Gly-Gly-Gly-Pro-$OCH_2Ph$ (1.80 g, 1.81 mmol, 1.0 equiv) was dissolved in hot EtOH (80 mL), 10% Pd/C (0.55 g) was added (Parr shaker), and the suspension was shaken (60 psi H_2, 3 h, RT, monitored by TLC 95:5 CH_2Cl_2/MeOH). The mixture was filtered (celite) and evaporated in vacuo to give white solid (1.69 g, 99%). ^{1}H NMR: δ=0.87 (t, J=7.0 Hz, 6H; CH_2CH_3), 1.25 (brs, 60H; $NCH_2CH_2(CH_2)_{15}CH_3$), 1.51 (brs, 4H; $NCH_2CH_2(CH_2)_{15}CH_3$), 1.98–2.22 (m, 4H; Pro $NCH_2CH_2CH_2$), 3.09 (t, J=7.4 Hz, 2H; $NCH_2CH_2(CH_2)_{15}CH_3$), 3.27 (t, J=7.5 Hz, 2H; $NCH_2CH_2(CH_2)_{15}CH_3$), 3.52–3.73 (m, 2H; Pro $NCH_2CH_2CH_2$), 3.94–4.39 (m, 9H; Gly CH_2, Pro CH, $COCH_2O$), 7.75 (brs, 1H; NH), 8.00 (brs, 1H; NH), 8.24 ppm (brs, 1H; NH); ^{13}C NMR: δ=14.3, 22.9, 25.1, 27.1, 27.3, 27.8, 29.0, 29.5, 29.6, 29.8, 29.9, 29.9, 32.1, 42.0, 43.1, 46.7, 47.3, 60.0, 69.4, 71.3, 168.3, 169.1, 170.1, 170.4, 171.4, 173.9 ppm.

$(C_{18}H_{37})_2NCOCH_2OCH_2CO$-Gly-Gly-Gly-Pro-Phe-OBz: L-Phenylalanine benzyl ester tosylate salt (0.24 g, 0.55 mmol, 1 equiv) was dissolved in dry CH_2Cl_2 and cooled to 0°C under N_2. $(C_{18}H_{37})_2NCOCH_2OCH_2CO$-Gly-Gly-Gly-Pro-OH (0.50 g, 0.55 mmol), EDCI (0.12 g, 0.61 mmol), HOBt (0.08 g, 0.61 mmol) and NEt_3 (dropwise, 0.17 g, 1.66 mmol) was added to this solution. The reaction was stirred (0°C, 30 min then RT 48 h). The solvent was evaporated in vacuo and the resulting yellow oil was subjected to chromatography (silica gel, 97:3 CH_2Cl_2/MeOH) to afford a white solid (0.50 g, 78%). ^{1}H NMR: δ=0.88 (t, J=6.9 Hz, 6H; CH_2CH_3), 1.25 (brs, 60H; $NCH_2CH_2(CH_2)_{15}CH_3$), 1.49 (brs, 4H; $NCH_2CH_2(CH_2)_{15}CH_3$), 1.79–1.82 (m, 4H; Pro $NCH_2CH_2CH_2$), 2.96–3.41 (m, 6H; $NCH_2CH_2(CH_2)_{15}CH_3$, Phe $NHCH(CH_2C_6H_5)CO$), 3.93–4.13 (m, 8H; Gly CH_2, $COCH_2O$), 4.30 (s, 2H; $COCH_2O$), 4.52 (m, 2H; Phe NHCH), 4.83 (q, J=5.9 Hz, 1H; Pro CH), 5.15 (m, 2H; Pro $NCH_2CH_2CH_2$), 5.29 (s, 2H; $OCH_2C_6H_5$), 7.07–7.40 (m, 12H; $COOCH_2C_6H_5$, $NHCH(CH_2C_6H_5)CO$, NH, NH), 7.73 (t, J=5.8 Hz, 1H; NH), 8.29 ppm (bt, J=5.7 Hz, 1H; NH); ^{13}C NMR: δ=14.3, 22.9, 24.7, 27.1, 27.3, 27.8, 29.1, 29.5, 29.6, 29.6, 29.7, 29.8, 29.9, 32.1, 37.8, 43.2, 46.6, 47.0, 53.4, 53.6, 60.1, 67.3, 69.9, 127.1, 128.5, 128.6, 128.6, 128.8, 129.5, 135.5, 136.4, 142.4, 168.2, 168.7, 169.4, 170.0, 171.3, 171.7 ppm.

$(C_{18}H_{37})_2NCOCH_2OCH_2CO$-Gly-Gly-Gly-Pro-Phe-OH: $(C_{18}H_{37})_2NCOCH_2OCH_2CO$-Gly-Gly-Gly-Pro-Phe-$OCH_2Ph$ (0.46 g, 0.40 mmol) in hot EtOH (40 mL) and 10% Pd/C (0.14 g) were placed in a Parr shaker. The suspension was shaken (60 psi H_2, 3 h), the mixture was filtered (celite pad) and the solvent was evaporated to give a white solid (0.42 g, 98%). ^{1}H NMR: δ=0.88 (t, J=6.9 Hz, 6H; CH_2CH_3), 1.25 (brs, 60H; $NCH_2CH_2(CH_2)_{15}CH_3$), 1.50 (brs, 4H; $NCH_2CH_2(CH_2)_{15}CH_3$), 1.82–1.92 (m, 4H; Pro $NCH_2CH_2CH_2$), 3.04–3.49 (m, 6H; $NCH_2CH_2(CH_2)_{15}CH_3$, Phe $NHCH(CH_2C_6H_5)CO$), 3.71–4.12 (m, 8H; Gly CH_2, $COCH_2O$), 4.28 (s, 2H; $COCH_2O$), 4.47 (m, 2H; Phe NHCH), 4.82 (q, J=5.9 Hz, 1H; Pro CH), 5.15 (m, 2H; Pro $NCH_2CH_2CH_2$), 5.29 (s, 2H; $OCH_2C_6H_5$), 7.17–7.25 (m, 5H; $NHCH(CH_2C_6H_5)CO$), 7.70 (brs, 1H; NH), 7.84 (brs, 1H; NH), 8.24 (brs, 1H; NH), 8.33 ppm (brs, 1H; NH); ^{13}C NMR: δ=14.3, 22.9, 27.1, 27.2, 27.8, 29.0, 29.6, 29.6, 29.8, 29.9, 32.1, 43.2, 46.7, 47.2, 53.6, 126.9, 128.5, 129.6, 168.8, 170.2, 170.4, 170.6, 170.9, 171.3 ppm.

*$(C_{18}H_{37})_2NCOCH_2OCH_2CO$-Gly-Gly-Gly-Pro-Phe-Gly-Gly-OC_7H_{15} (**3**)*: $(C_{18}H_{37})_2NCOCH_2OCH_2CO$-Gly-Gly-Gly-Pro-Phe-OH (0.40 g, 0.38 mmol) was added under N_2 to dry CH_2Cl_2 (40 mL) and cooled to 0°C. Diglycyl heptyl ester tosylate salt (TsOH·Gly-Gly-OC_7H_{15}) (0.15 g, 0.38 mmol; for synthesis see reference [24]), EDCI (0.08 g, 0.42 mmol), HOBt (0.06 g, 0.42 mmol), and NEt_3 (0.12 g, 1.14 mmol) were added. The reaction was stirred (0°C for 30 min, 48 h at RT). The solvent was evaporated in vacuo, the resulting yellow oil was subjected to chromatography (silica gel, 93:7 CH_2Cl_2/MeOH), and the product crystallized from MeOH to afford a white solid (0.46 g, 95%). M.p. 118–120°C; ^{1}H NMR: δ=0.88 (t, J=6.9 Hz, 9H; CH_2CH_3), 1.25 (brs, 68H; $NCH_2CH_2(CH_2)_{15}CH_3$, $OCH_2CH_2(CH_2)_4CH_3$), 1.50–1.62 (m, 6H; $NCH_2CH_2(CH_2)_{15}CH_3$ and $OCH_2CH_2(CH_2)_4CH_3$), 1.65–2.06 (m, 4H; Pro $NCH_2CH_2CH_2$), 3.00–3.08 (m, 3H; $NCH_2CH_2(CH_2)_{15}CH_3$, Pro CH), 3.28–3.63 (m, 4H; $NCH_2CH_2(CH_2)_{15}CH_3$, $OCH_2CH_2(CH_2)_4CH_3$), 3.69–3.80 (m, 4H; Pro NCH_2CH_2, Phe $NHCH(CH_2C_6H_5)$), 3.91–4.22 (m, 12H; 10H= Gly CH_2, $COCH_2O$), 4.30 (s, 2H; $COCH_2O$), 4.55 (m, 1H; Phe NHCH), 7.09 (brs, 1H; NH), 7.20–7.32 (m, 5H; Phe C_6H_5), 7.41 (t, J=5.0 Hz, 1H; NH), 7.55 (t, J=6.0 Hz, 1H; NH), 7.75 (t, J=5.0 Hz, 1H; NH), 7.83 (t, J=6.2 Hz, 1H; NH), 8.55 ppm (brs, 1H; NH); ^{13}C NMR: δ=14.3, 22.8, 22.9, 24.6, 26.0, 27.1, 27.3, 27.9, 28.7, 29.1, 29.3, 29.5, 29.6, 29.8, 29.8, 29.9, 31.9, 32.1, 36.2, 41.5, 42.6, 43.1, 43.7, 46.6, 41.2, 47.7, 55.1, 61.7, 65.9, 70.0, 72.1, 77.4, 126.8, 128.6, 129.0, 129.4, 138.2, 168.7, 169.8, 170.2, 170.4, 170.6, 171.0, 171.6, 172.0, 172.0, 172.5 ppm; ES-MS: m/z (%): 1265.9 (100).

Compound 4

Boc-W(N-CHO)GG-OC_7H_{15}: Boc-W(N-CHO)-OH (0.50 g, 1.50 mmol), glycylglycine *n*-heptyl ester tosylate[29] (0.61 g, 1.50 mmol), EDCI (0.32 g, 1.66 mmol) and HOBt (0.22 g, 1.66 mmol) were dissolved in CH_2Cl_2 (30 mL), cooled at 0°C, and Et_3N (0.63 mL) was added. The mixture was stirred (24 h, RT), the solvent was evaporated in vacuo, the residue was subjected to chromatography (silica gel, $CHCl_3$/MeOH=98:2) to afford an oil (0.55 g, 67%). ^{1}H NMR: δ=0.88 (t, J=6.8 Hz, 3H; CH_2CH_3), 1.20–1.33 (m, 8H; $OCH_2CH_2(CH_2)_4CH_3$), 1.38 (s, 9H; $C(CH_3)_3$), 1.62 (quint, J=7.0 Hz, 2H; $OCH_2CH_2(CH_2)_4CH_3$), 3.10–3.32 (m, 2H; Trp CH_2), 3.85–4.05 (m, 4H; Gly CH_2), 4.10 (t, J=6.9 Hz, 2H; $OCH_2CH_2(CH_2)_4CH_3$), 4.52 (brs, 1H; Trp CH), 5.44 (brs, 1H; NH), 6.90–9.10 ppm (m, 8H; CONH, indole CH and CHO); ^{13}C NMR: δ=14.2, 22.7, 25.9, 28.0, 28.4, 28.7, 29.0, 31.9, 41.4, 43.2, 54.7, 66.0, 80.8, 116.4, 119.2, 124.0, 124.8, 125.7, 155.9, 159.7, 169.1, 170.0, 172.2 ppm.

Boc-PW(N-CHO)GG-OC_7H_{15}: Boc-W(N-CHO)GG-OC_7H_{15} (0.53 g, 0.97 mmol) was deprotected in 4N HCl/dioxane (RT, 2 h). HCl·W(N-CHO)GG-OC_7H_{15}, Boc-Pro-OH (0.21 g, 0.97 mmol), EDCI (0.20 g, 1.07 mmol) and HOBt (0.14 g, 1.07 mmol) were dissolved in CH_2Cl_2 (30 mL), cooled at 0°C, Et_3N (0.41 mL) was added, and the mixture was warmed to RT (48 h). The solvent was evaporated in vacuo and the residue was subjected to chromatography (silica gel, $CHCl_3$/MeOH=98:2) to give a white solid (0.44 g, 70%). ^{1}H NMR: δ=0.88 (t, J=6.7 Hz, 3H; CH_2CH_3), 1.15–1.45 (m, 17H; $OCH_2CH_2(CH_2)_4CH_3$ and $C(CH_3)_3$), 1.55–2.20 (m, 6H; $OCH_2CH_2(CH_2)_4CH_3$ and Pro $NCH_2CH_2CH_2$), 2.80–3.50 (m, 4H; Trp CH_2 and Pro $NCH_2CH_2CH_2$), 3.80–4.20 (m, 7H; Gly CH_2, $OCH_2CH_2(CH_2)_4CH_3$ and Pro CH), 4.80 (brq, J=6.7 Hz, 1H; Trp CH), 6.70–9.20 ppm (m, 9H; CONH, indole CH and CHO); ^{13}C NMR: δ= 14.3, 22.8, 24.8, 26.0, 28.3, 28.7, 29.1, 29.7, 31.9, 41.5, 43.5, 47.4, 53.7, 61.1, 65.8, 81.3, 116.7, 118.6, 124.9, 125.8, 131.6, 134.5, 156.0, 160.0, 169.3, 169.9, 171.8, 173.0 ppm.

*$(C_{18}H_{37})_2NCOCH_2OCH_2CO$-Gly-Gly-Gly-Pro-(L)-Trp-Gly-Gly-OC_7H_{15} (**4**)*: Boc-PW(N-CHO)GG-OC_7H_{15} (0.42 g, 0.65 mmol) was deprotected (4N HCl/dioxane, RT, 2 h). HCl·PW(N-CHO)GG-OC_7H_{15}, $(C_{18}H_{37})_2NCOCH_2OCH_2CO$-GGG-OH[24] (0.53 g, 0.65 mmol), EDCI (0.14 g, 0.72 mmol) and HOBt (0.10 g, 0.72 mmol) were suspended in CH_2Cl_2 (30 mL), cooled at 0°C, Et_3N (0.27 mL) was added, and the mixture stirred at RT for 90 h. The solvent was evaporated, the residue was crystallized from MeOH, and further purified by chromatography (silica gel, $CHCl_3$/MeOH=95:5–90:10). The NMR spectra indicated that the product was a mixture of $(C_{18}H_{37})_2NCOCH_2OCH_2CO$-GGGPW(N-CHO)GG-$OC_7H_{15}$ and $(C_{18}H_{37})_2NCOCH_2OCH_2CO$-GGGPWGG-$OC_7H_{15}$ (0.36 g, 41%). A portion (0.15 g) was dissolved in THF, and NaOH (1.5 mL, 0.1 M) was added dropwise. The mixture was stirred at RT (40 min). Acetic acid was added (pH ca. 5) and the solvents evaporated. The residue was dissolved in CH_2Cl_2 (15 mL) at 0°C. EDCI (0.024 g, 0.12 mmol), DMAP (0.010 g, 0.08 mmol), and 1-heptanol (0.018 mL,

0.12 mmol) were added and the mixture stirred at RT for 24 h. Evaporation of the solvent followed by chromatography (silica gel, $CHCl_3$/MeOH = 93:7- 90:10) and crystallization from MeOH gave an off-white solid (0.14 g, 95%, two steps). ^{1}H NMR: δ = 0.88 (t, J = 6.6 Hz, 9H; CH_2CH_3), 1.15–1.40 (m, 68H; $NCH_2CH_2(CH_2)_{15}CH_3$ and OCH_2CH_2-$(CH_2)_4CH_3$), 1.41–1.67 (m, 6H; $NCH_2CH_2(CH_2)_{15}CH_3$ and OCH_2CH_2-$(CH_2)_4CH_3$), 1.72–2.10 (m, 4H; Pro $NCH_2CH_2CH_2$), 2.87–3.70 (m, 8H; $NCH_2CH_2(CH_2)_{15}CH_3$, Trp CH_2 and Pro $NCH_2CH_2CH_2$), 3.86–4.38 (m, 17H; Gly CH_2, Pro CH, $OCH_2CH_2(CH_2)_4CH_3$ and OCH_2CO), 4.61 (q, J = 5.8 Hz, 1H; Trp CH), 6.64 (d, J = 6.3 Hz, 1H; Trp $CONH$), 7.00–7.15 (m, 3H; indole CH and $CONH$), 7.18 (t, 1H; J = 7.6 Hz, indole CH), 7.33 (brt, J = 7.3 Hz, 1H; $CONH$), 7.41 (d, J = 8.1 Hz, 1H; indole CH), 7.45–7.57 (m, 2H; indole CH and $CONH$), 8.05 (brs, 1H; $CONH$), 8.46 (t, J = 5.7 Hz, 1H; $CONH$), 9.86 ppm (s, 1H; indole NH). ^{13}C NMR: δ = 14.2, 14.3, 22.8, 22.9, 24.8, 25.9, 26.0, 27.1, 27.3, 27.8, 28.7, 28.9, 29.0, 29.1, 29.4, 29.5, 29.6, 29.7, 29.8, 29.9, 31.9, 32.1, 41.5, 41.9, 43.1, 43.3, 46.6, 46.7, 47.1, 54.7, 61.6, 65.8, 69.8, 71.9, 108.2, 112.6, 117.7, 119.6, 122.1, 124.8, 128.0, 136.4, 168.9, 169.0, 169.8, 170.1, 170.4, 170.7, 171. 172.4 ppm; elemental analysis calcd (%) for $C_{73}H_{125}N_9O_{11}$: C 67.20, H 9.66, N 9.66; found: C 67.12, H 9.53, N 9.59.

Compound 5

Boc-(D)-Trp-Gly-Gly-OC_7H_{15}: Boc-(D)-Tryptophan (0.25 g, 0.82 mmol) was dissolved in dry CH_2Cl_2 (30 mL), cooled to 0°C and diglycyl heptyl ester tosylate salt[29] (TsOH·Gly-Gly-OC_7H_{15}, 0.33 g, 0.82 mmol), EDCI (0.17 g, 0.90 mmol, HOBt (0.12 g, 0.90 mmol, and NEt_3 (0.25 g, 2.46 mmol) were added. The reaction was stirred at 0°C for 30 min and then at RT for 24 h. The solvent was evaporated, the resulting yellow oil was subjected to chromatography (silica gel, 98:2 CH_2Cl_2/MeOH), and the residue was crystallized from MeOH to afford an off-white solid (0.25 g, 59%). ^{1}H NMR: δ = 0.88 (t, J = 6.8 Hz, 3H; OCH_2CH_2-$(CH_2)_4CH_3$), 1.29 (brs, 8H; $OCH_2CH_2(CH_2)_4CH_3$), 1.40 (s, 9H; $(CH_3)_3$), 1.62 (m, 2H; $OCH_2CH_2(CH_2)_4CH_3$), 3.22 (m, 2H; Gly CH_2), 3.81–3.87 (m, 4H; Gly CH_2, indole CH_2), 4.10 (t, J = 6.7 Hz, 2H; OCH_2CH_2-$(CH_2)_4CH_3$), 4.40 (m, 1H; Trp CH), 5.24 (brs, 1H; NH), 6.63 (brs, 1H; NH), 7.06–7.18 (m, 3H; indole aromatic CH), 7.32–7.35 (m, 1H; indole aromatic CHNH), 7.58–7.60 (m, 1H; indole aromatic CHNH), 8.49 ppm (brs, 1H; NH). ^{13}C NMR: δ = 14.3, 22.8, 25.9, 28.5, 28.7, 29.1, 31.9, 41.3, 43.2, 65.9, 77.4, 110.3, 111.6, 118.9, 119.9, 122.5, 123.6, 127.5, 136.4, 169.8, 169.9, 172.8 ppm.

$(C_{18}H_{37})_2NCOCH_2OCH_2CO$-Gly-Gly-Gly-Pro-(D)-Trp-Gly-Gly-OC_7H_{15} (***5***): Boc-(D)-WGG-OC_7H_{15} (0.30 g, 0.61 mmol) was stirred with 4N HCl/dioxane for 2 h. HCl·(D)-WGG-OC_7H_{15}, $(C_{18}H_{37})_2NCOCH_2OCH_2CO$-GGGP-OH (0.53 g, 0.61 mmol, see above for synthesis), EDCI (0.13 g, 0.68 mmol) and HOBt (0.09 g, 0.68 mmol) were suspended in CH_2Cl_2 (30 mL). The mixture was cooled to 0°C, Et_3N (0.19 g) was added, and stirring was continued at RT for 3 d. Evaporation of the solvent and chromatography (silica gel, $CHCl_3$/MeOH = 93:7) followed by crystallization from MeOH gave an off-white solid (0.35 g, 48%). ^{1}H NMR: δ = 0.87 (t, J = 6.8 Hz, 9H; CH_2CH_3), 1.25–1.61 (m, 74H; NCH_2CH_2-$(CH_2)_{15}CH_3$, $OCH_2CH_2(CH_2)_4CH_3$, $NCH_2CH_2(CH_2)_{15}CH_3$ and $OCH_2CH_2(CH_2)_4CH_3$), 1.85–2.04 (m, 4H; Pro $NCH_2CH_2CH_2$), 3.06 (t, J = 7.8 Hz, 2H; $NCH_2CH_2(CH_2)_{15}CH_3$), 3.24–3.52 (m, 9H; NCH_2CH_2-$(CH_2)_{15}CH_3$, Trp CH_2, Pro $NCH_2CH_2CH_2$, $OCH_2CH_2(CH_2)_4CH_3$, Pro CH), 3.67–4.26, (m, 14H; Gly CH_2, OCH_2CO), 4.59 (q, J = 5.5 Hz, 1H; Trp CH), 7.04–7.44 (m, 6H; indole CH, NH), 7.57 (d, J = 7.8 Hz, 1H; Trp CONH), 7.79 (t, J = 5.8 Hz, 1H; NH), 7.87 (t, J = 5.8 Hz, 1H; NH), 8.30 (t, J = 5.8 Hz, 1H; NH), 9.18 ppm (1H; s, indole CH);^{13}C NMR: δ = 14.2, 14.3, 22.8, 22.9, 25.4, 26.0, 26.5, 27.1, 27.3, 27.8, 29.1, 29.6, 31.9, 32.1, 41.4, 41.8, 43.2, 46., 47.1, 51.0, 55.1, 61.2, 65.9, 69.6, 71.6, 109.7, 111.8, 118.6, 119.7, 122.2, 123.9, 127.8, 136.5, 168.6, 170.1, 170.3, 170.4, 171.0, 172.2, 173.4 ppm.

Compound 6

Boc-AG-OC_7H_{15}: TsOH·Gly-OC_7H_{15}[29] (0.51 g, 1.49 mmol), Boc-L-Ala (0.28 g, 1.48 mmol), EDCI (0.31 g, 1.62 mmol) and HOBt (0.22 g, 1.63 mmol) were dissolved in CH_2Cl_2 (40 mL) and Et_3N (0.61 mL) was added. The mixture was stirred at 0°C for 0.5 h and then at RT for 48 h. The solvent was evaporated and the residue was dissolved in CH_2Cl_2 (40 mL), washed with 5% citric acid (2×20 mL), H_2O (2×20 mL), 5% $NaHCO_3$ (2×20 mL), brine (2×20 mL), dried over $MgSO_4$ and the solvent was evaporated. The residue was subjected to chromatography (silica gel, EtOAc/hexane = 40: 60) to give an oil (0.42 g, 83%). ^{1}H NMR: δ = 0.87 (t, J = 6.3 Hz, 3H; CH_2CH_3), 1.20–1.35 (m, 8H; $OCH_2CH_2(CH_2)_4CH_3$), 1.37 (d, J = 7.2 Hz, 3H; Ala CH_3), 1.44 (s, 9H; C-$(CH_3)_3$), 1.63 (quint, J = 6.6 Hz, 2H; $OCH_2CH_2(CH_2)_4CH_3$), 4.02 (d, J = 5.1 Hz, 2H; Gly CH_2), 4.13 (t, J = 6.8 Hz, 2H; $OCH_2CH_2(CH_2)_4CH_3$), 4.23 (br quint, J = 6.6 Hz, 1H; Ala CH), 5.11 (d, J = 6.6 Hz, 1H; Ala NH), 6.79 ppm (brs, 1H; Gly NH); ^{13}C NMR: δ = 14.2, 18.5, 22.8, 26.0, 28.5, 28.7, 29.0, 31.9, 41.5, 65.9, 80.5, 100.2, 170.0, 173.0 ppm; IR (KBr): $\tilde{\nu}$ = 3320, 3088, 2958, 2932, 2859, 1753, 1715, 1668, 1531, 1455, 1392, 1367, 1291, 1250, 1172, 1068, 1048, 1028 cm^{-1}.

Boc-GAG-OC_7H_{15}: Boc-AG-OC_7H_{15} was treated with 4N HCl in dioxane for 1 h. HCl·AG-OC_7H_{15} (0.49 g, 1.75 mmol), Boc-Gly-OH (0.31 g, 1.75 mmol), EDCI (0.37 g, 1.92 mol) and HOBt (0.26 g, 1.92 mmol) were dissolved in CH_2Cl_2 (30 mL) and Et_3N (0.73 mL) was then added. The mixture was stirred at 0°C for 0.5 h and at RT for 12 h. The solvent was removed in vacuo. The residue was dissolved in CH_2Cl_2 (40 mL), washed with 5% citric acid (2×20 mL), H_2O (2×20 mL), 5% $NaHCO_3$ (2×20 mL), brine (2×20 mL), dried over $MgSO_4$ and the solvent was evaporated. Chromatography (silica gel, $CHCl_3/CH_3OH$ = 97:3) gave an oil (0.50 g, 71%). ^{1}H NMR: δ = 0.88 (t, J = 6.3 Hz, 3H; CH_2CH_3), 1.30 (pseudo-s, 8H; $OCH_2CH_2(CH_2)_4CH_3$), 1.41 (d, J = 6.9 Hz, 3H; Ala CH_3), 1.45 (s, 9H; $C(CH_3)_3$), 1.64 (quint, J = 6.2 Hz, 2H; $OCH_2CH_2(CH_2)_4CH_3$), 3.83 (pseudo-s, 2H; Gly CH_2), 4.01 (t, J = 5.0 Hz, 2H; Gly CH_2), 4.13 (t, J = 6.8 Hz, 2H; $OCH_2CH_2(CH_2)_4CH_3$), 4.60 (quint, J = 7.0 Hz, 1H; Ala CH), 5.33 (1H; brs, Gly NH), 6.88 (1H; d, J = 7.5 Hz, Ala NH), 6.99 ppm (1H; brs, Gly NH); ^{13}C NMR: δ = 14.2, 18.3, 22.8, 26.0, 28.5, 28.7, 29.0, 31.9, 41.5, 44.5, 48.9, 65.9, 80.6, 169.8, 170.0, 172.5 ppm; IR (KBr): $\tilde{\nu}$ = 3310, 3076, 2958, 2932, 2859, 1743, 1717, 1658, 1529, 1455, 1392, 1367, 1283, 1249, 1174, 1052, 1021 cm^{-1}.

Boc-PGAG-OC_7H_{15}: Boc-GAG-OC_7H_{15} was stirred with 4N HCl in dioxane for 1 h. HCl·GAG-OC_7H_{15} (0.40 g, 1.18 mmol), Boc-Pro-OH (0.25 g, 1.18 mmol), EDCI (0.25 g, 1.30 mmol) and HOBt (0.18 g, 1.30 mmol) were dissolved in CH_2Cl_2 (35 mL) and Et_3N (0.50 mL) was added. The mixture was stirred at 0°C for 0.5 h and at RT for 48 h. Evaporation of the solvent and chromatography (silica gel, $CHCl_3/CH_3OH$ = 97:3) afforded a light yellow solid (0.51 g, 86%). M.p. 159–161°C; ^{1}H NMR: δ = 0.89 (t, J = 6.6 Hz, 3H; CH_2CH_3), 1.20–1.38 (m, 8H; $OCH_2CH_2(CH_2)_4CH_3$), 1.40–1.50 (m, 12H; Ala CH_3 and $C(CH_3)_3$), 1.82–2.22 (m, 4H; Pro $NCH_2CH_2CH_2$), 3.40–3.52 (m, 2H; Pro $NCH_2CH_2CH_2$), 3.93–4.02 (m, 4H; two Gly CH_2), 4.12 (t, J = 6.6 Hz, 2H; $OCH_2CH_2(CH_2)_4CH_3$), 4.21 (dd, J = 7.8, 5.4 Hz, 1H; Pro CH), 4.54 (quint, J = 7.4 Hz, 1H; Ala CH), 7.00 (brs, 2H; two Gly NH), 7.34 ppm (br d, J = 7.4 Hz, 1H; Ala NH); ^{13}C NMR: δ = 14.3, 17.6, 22.8, 25.3, 26.0, 28.6, 28.7, 29.1, 29.9, 31.9, 41.5, 43.2, 47.6, 49.4, 61.2, 65.7, 81.2, 173.7 ppm; IR (KBr): $\tilde{\nu}$ = 3307, 2957, 2930, 1752, 1668, 1535, 1454, 1407, 1367, 1165, 1133, 1019 cm^{-1}.

$(C_{18}H_{37})_2NCOCH_2OCH_2CO$-GGGPGAG-$OC_7H_{15}$ (***6***): Boc-PGAG-OC_7H_{15} was deprotected (4N HCl, dioxane, 1 h). $(C_{18}H_{37})_2NCOCH_2OCH_2CO$-GGG-OH (0.44 g, 0.54 mmol), HCl·PGAG-OC_7H_{15} (0.25 g, 0.54 mmol), EDCI (0.11 g, 0.60 mmol), and HOBt (0.08 g, 0.60 mmol) were suspended in CH_2Cl_2 (35 mL) and Et_3N (0.23 mL) was added. The mixture was stirred at 0°C for 0.5 h and at RT for 48 h. Evaporation of the solvent and chromatography (silica gel, $CHCl_3/CH_3OH/HOAc$ = 90: 10: 0.1) gave a white solid (0.19 g, 29%). M.p. 128–130°C; ^{1}H NMR: δ = 0.88 (t, J = 6.4 Hz, 9H; CH_2CH_3), 1.20–1.40 (m, 71H; $CH_3(CH_2)_{15}CH_2CH_2N$, $OCH_2CH_2(CH_2)_4CH_3$ and Ala CH_3), 1.42–1.67 (m, 6H; $CH_3(CH_2)_{15}CH_2CH_2N$ and OCH_2CH_2-$(CH_2)_4CH_3$), 1.92–2.21 (m, 4H; Pro $NCH_2CH_2CH_2$), 3.09 (t, 2H; J = 7.2 Hz, $CH_3(CH_2)_{15}CH_2CH_2N$), 3.28 (t, J = 7.5 Hz, 2H; CH_3-$(CH_2)_{15}CH_2CH_2N$), 3.50–3.80 (m, 3H; Pro $NCH_2CH_2CH_2$ and Gly CH_2), 3.85–4.15 (m, 13H; Gly CH_2, $COCH_2O$ and $OCH_2CH_2(CH_2)_4CH_3$), 4.29 (s, 2H; $COCH_2O$), 4.40–4.51 (m, 2H; Pro CH and Ala CH). 7.38–7.50 (m, 2H; two CONH), 7.54 (brt, J = 5.8 Hz, 1H; CONH), 7.90–8.02 (m, 2H; two CONH), 8.26 ppm (brt, J = 5.8 Hz, 1H; CONH); ^{13}C NMR: δ = 14.3, 17.7, 20.8, 22.8, 22.9, 25.3, 26.0, 27.1, 27.3, 27.8, 28.7, 29.1, 29.5, 29.6, 29.8, 29.9, 31.9, 32.1, 41.5, 43.2, 46.6, 47.2, 49.2, 51.2, 61.3, 65.8, 69.8, 71.8, 76.2, 100.2, 164.9, 168.2, 168.8, 169.7, 170.2, 170.3, 171.5, 172.8,

173.3 ppm; IR (KBr): $\tilde{\nu}$ = 3307, 3081, 2923, 2853, 1749, 1657, 1549, 1466, 1377, 1243, 1201, 1130, 1026, 721, 666 cm^{-1}.

Compound 7: $(C_{18}H_{37})_2NCOCH_2OCH_2CO$-Gly-Gly-Gly-Pro-Gly-Glu-Gly-OC_7H_{15} (**7**) was prepared as previously reported.[29]

Compound 8

Boc-W(N-CHO)G-OC_7H_{15}: Boc-W(N-CHO)-OH (0.60 g, 1.80 mmol), glycine *n*-heptyl ester tosylate[29] (0.62 g, 1.80 mmol), EDCI (0.38 g, 1.99 mmol) and HOBt (0.27 g, 1.99 mmol) were dissolved in CH_2Cl_2 (35 mL), and cooled to 0 °C. Et_3N (0.75 mL) was added and the mixture was stirred at RT for 72 h. Evaporation of the solvent and chromatography (silica gel, hexane/EtOAc = 2:1) afforded an oil (0.62 g, 70 %). ^{1}H NMR: δ = 0.88 (t, J = 6.7 Hz, 3H; CH_2CH_3), 1.20–1.36 (m, 8H; $OCH_2CH_2(CH_2)_4CH_3$), 1.39 (s, 9H; $C(CH_3)_3$), 1.50–1.70 (m, 2H; $OCH_2CH_2(CH_2)_4CH_3$), 3.10–3.33 (m, 2H; Trp CH_2), 3.96 (d, J = 5.3 Hz, 2H; Gly CH_2), 4.09 (t, J = 6.8 Hz, 2H; $OCH_2CH_2(CH_2)_4CH_3$), 4.57 (brs, 1H; Trp *CH*), 5.29 (d, J = 8.2 Hz, 1H; *NH*), 6.65–9.10 ppm (m, 7H; *CONH*, indole *CH* and *CHO*); ^{13}C NMR: δ = 14.2, 22.7, 25.9, 28.4, 28.6, 29.0, 31.8, 41.4, 54.3, 65.9, 80.6, 116.4, 118.6, 119.2, 124.1, 124.8, 125.6, 131.4, 134.5, 155.6, 159.6, 169.7, 171.6 ppm.

Boc-GW(N-CHO)G-OC_7H_{15}: Boc-W(N-CHO)G-OC_7H_{15} (0.60 g, 1.23 mmol) was deprotected (4N HCl/dioxane, 2 h). HCl·W(N-CHO)G-OC_7H_{15}, Boc-Gly-OH (0.22 g, 1.23 mmol), EDCI (0.26 g, 1.35 mmol) and HOBt (0.18 g, 1.35 mmol) were dissolved in CH_2Cl_2 (35 mL), cooled at 0 °C and Et_3N (0.51 mL) was added. The mixture was stirred at RT for 72 h. Evaporation of the solvent and chromatography (silica gel, $CHCl_3$/MeOH = 98:2) gave an oil (0.42 g, 63 %). ^{1}H NMR: δ = 0.88 (t, J = 6.5 Hz, 3H; CH_2CH_3), 1.20–1.34 (m, 8H; $OCH_2CH_2(CH_2)_4CH_3$), 1.37 (s, 9H; $C(CH_3)_3$), 1.50–1.71 (m, 2H; $OCH_2CH_2(CH_2)_4CH_3$), 3.13–3.31 (m, 2H; Trp CH_2), 3.74–4.00 (m, 4H; Gly CH_2), 4.07 (t, J = 6.6 Hz, 2H; $OCH_2CH_2(CH_2)_4CH_3$), 4.91 (d, J = 7.0 Hz, 1H; Trp *CH*), 5.36 (brs, 1H; *NH*), 7.00–9.10 ppm (m, 8H; *CONH*, indole *CH* and *CHO*); ^{13}C NMR: δ = 14.4, 22.9, 26.1, 27.9, 28.6, 28.9, 29.2, 32.0, 41.6, 44.8, 53.1, 66.1, 80.8, 116.6, 118.3, 119.2, 124.8, 124.9, 125.7, 131.6, 134.6, 156.7, 160.2, 170.0, 170.4, 171.6 ppm.

Boc-PGW(N-CHO)G-OC_7H_{15}: Boc-GW(N-CHO)G-OC_7H_{15} (0.35 g, 0.64 mmol) was deprotected (4N HCl/dioxane, 2 h). HCl·GW(N-CHO)G-OC_7H_{15}, Boc-Pro-OH (0.14 g, 0.64 mmol), EDCI (0.14 g, 0.71 mmol), and HOBt (0.095 g, 0.71 mmol) were dissolved in CH_2Cl_2 (25 mL), cooled at 0 °C and Et_3N (0.27 mL) was added. The mixture was stirred at RT for 64 h. Evaporation of the solvent and chromatography (silica gel, $CHCl_3$/MeOH = 98:2) gave an oil (0.31 g, 75 %). ^{1}H NMR: δ = 0.88 (t, J = 6.8 Hz, 3H; CH_2CH_3), 1.15–1.45 (m, 17H; $OCH_2CH_2(CH_2)_4CH_3$ and $C(CH_3)_3$), 1.50–2.18 (m, 6H; $OCH_2CH_2(CH_2)_4CH_3$ and Pro $NCH_2CH_2CH_2$), 3.08–3.53 (m, 4H; Trp CH_2 and Pro $NCH_2CH_2CH_2$), 3.72–4.25 (m, 7H; Gly CH_2, $OCH_2CH_2(CH_2)_4CH_3$ and Pro *CH*), 4.86 (brs, 1H; Trp *CH*), 6.80–9.20 ppm (m, 9H; *CONH*, indole *CH* and *CHO*); ^{13}C NMR: δ = 14.2, 22.8, 24.8, 26.0, 27.2, 28.5, 28.7, 29.1, 29.6, 31.9, 41.5, 43.7, 47.6, 53.0, 60.8, 65.8, 81.0, 116.3, 119.1, 124.7, 125.5, 131.5, 134.5, 155.8, 160.1, 169.9, 171.4, 173.9 ppm.

*$(C_{18}H_{37})_2NCOCH_2OCH_2CO$-Gly-Gly-Gly-Pro-Gly-L-Trp-Gly-OC_7H_{15} (**8**)*: Boc-PGW(N-CHO)G-OC_7H_{15} (0.30 g, 0.47 mmol) was deprotected (4N HCl/dioxane, 2 h). HCl·PGW(N-CHO)G-OC_7H_{15}, $(C_{18}H_{37})_2NCOCH_2OCH_2CO$-GGG-OH (0.38 g, 0.47 mmol), EDCI (0.098 g, 0.51 mmol), and HOBt (0.069 g, 0.51 mmol) were suspended in CH_2Cl_2 (25 mL) and Et_3N (0.20 mL) was added (0 °C). The mixture was stirred at RT for 60 h. The solvent was evaporated and the residue was crystallized from MeOH. Chromatography (silica gel, $CHCl_3$:MeOH = 98:2–95: 5–93:7) afforded two major fractions. The first fraction was reduced in volume and crystallized from MeOH to afford a white solid (130 mg, 21 %) identified as $(C_{18}H_{37})_2NCOCH_2OCH_2CO$-GGGPGW(N-CHO)G-$OC_7H_{15}$. ^{1}H NMR (300 MHz; all peaks were broad): δ = 0.88 (t, J = 6.9 Hz, 9H; CH_2CH_3), 1.00–1.71 (m, 74H; $NCH_2(CH_2)_{16}CH_3$ and $OCH_2(CH_2)_5CH_3$), 1.75–2.28 (m, 4H; Pro $NCH_2CH_2CH_2$), 2.93–4.50 (m, 25H; $NCH_2CH_2(CH_2)_{15}CH_3$, Trp CH_2, Pro $NCH_2CH_2CH_2$, Gly CH_2, $OCH_2CH_2(CH_2)_4CH_3$, Pro *CH* and OCH_2CO), 4.80 (brs, 1H; Trp *CH*), 7.20–8.45 (m, 11H; indole *CH* and *CONH*), 9.11 ppm s, (1H; *CHO*); ^{13}C NMR ($CDCl_3$): δ = 14.2, 14.3, 22.8, 22.9, 25.2, 26.0, 26.8, 27.1, 27.2, 27.8, 28.7, 29.1, 29.5, 29.6, 29.7, 29.8, 29.9, 31.9, 32.1, 41.5, 41.9, 42.9, 43.3, 43.6, 46.5, 47.1, 53.0, 61.1, 65.8, 69.7, 71.7, 116.1, 118.5, 119.2, 124.5, 124.6, 125.3, 131.6, 134.2, 160.6, 168.5, 168.7, 170.1, 171.5, 171. 173.0 ppm; elemental analysis calcd (%) for $C_{74}H_{125}N_9O_{12}$: C 66.68, H 9.45, N 9.46; found: C 66.82, H 9.30, N 9.20.

Fraction 2 was reduced to minimum volume and crystallized from MeOH to give an off-white solid (80 mg, 13 %). This fraction was identified as $(C_{18}H_{37})_2NCOCH_2OCH_2CO$ -GGGPGWG-OC_7H_{15}. ^{1}H NMR (300 MHz; all peaks were broad): δ = 0.88 (t, J = 7.0 Hz, 9H; CH_2CH_3), 1.10–1.70 (m, 74H; $NCH_2(CH_2)_{16}CH_3$ and $OCH_2(CH_2)_5CH_3$), 1.80–2.20 (m, 4H; Pro $NCH_2CH_2CH_2$), 2.93–4.50 (m, 25H; $NCH_2CH_2(CH_2)_{15}CH_3$, Trp CH_2, Pro $NCH_2CH_2CH_2$, Gly CH_2, $OCH_2CH_2(CH_2)_4CH_3$, Pro *CH* and OCH_2CO), 4.78 (brs, 1H; Trp *CH*), 6.95–8.30 (m, 11H; indole *CH* and *CONH*), 9.53 ppm (s, 1H; indole *NH*); ^{13}C NMR: δ = 14.2, 14.3, 22.8, 22.9, 24.9, 26.0, 27.1, 27.3, 27.8, 28.7, 29.1, 29.5, 29.6, 29.8, 29.9, 31.9, 32.1, 41.5, 42.2, 42.8, 46.6, 46.8, 47.2, 54.1, 61.1, 65.6, 69.7, 71.6, 110.6, 111.9, 118.7, 118.9, 121.6, 124.4, 127.6, 136.6, 168.5, 168.6, 170.0, 170.2, 170.4, 170.5, 171.2, 172. 173.1 ppm; elemental analysis calcd (%) for $C_{73}H_{125}N_9O_{11}$: C 67.20, H 9.66, N 9.66; found: C 67.42, H 9.41, N 9.47.

Compound 9: $(C_{18}H_{37})_2NCOCH_2OCH_2CO$-Gly-Gly-Gly-Pro-Gly-Gly-Glu(OBz)-OC_7H_{15} (**9**) was prepared as reported.[29]

Compound 10: $(C_{18}H_{37})_2NCOCH_2OCH_2CO$-Gly-Gly-Gly-Pro-Gly-Gly-Glu(OCH_2pyrene)-OC_7H_{15} (**10**) was prepared as previously reported.[29]

Compound 11: $(C_{18}H_{37})_2NCOCH_2OCH_2CO$-Gly-Gly-Gly-Pro-Gly-Gly-Lys(NBD)-OC_7H_{15} (**11**) was prepared as previously reported.[29]

Compounds 12 and **13**

N-*Formyl* L-*tryptophan* n-*heptyl ester tosylate*: A mixture of L-Trp(N-CHO)-OH (0.60 g, 2.75 mmol), $TsOH·H_2O$ (0.58 g, 3.02 mmol), 1-heptanol (3.1 mL, 22.0 mmol), and toluene (40 mL) was heated to reflux and water removed (Dean–Stark) during 10 h. The mixture was cooled to RT, Et_2O (200 mL) was added, and the mixture was further cooled to 0 °C (16 h). Filtration gave a white solid (0.78 g, 58 %). ^{1}H NMR: δ = 0.88 (t, J = 6.9 Hz, 3H; CH_2CH_3), 1.00–1.45 (m, 10H; $OCH_2(CH_2)_5CH_3$), 2.31 (s, 3H; $CH_3C_6H_4SO_3$), 3.30–3.40 (m, 2H; Trp CH_2), 3.49 (s, 3H; indole NCH_3), 3.73–3.98 (m, 3H; $OCH_2CH_2(CH_2)_4CH_3$ and Trp *CH*), 6.96–7.30 (m, 6H; indole *CH* and H_{Ar}), 7.42 (d, J = 7.8 Hz, 1H; indole *CH*), 7.60 (d, J = 7.8 Hz, 2H; H_{Ar}), 8.13 ppm (brs, 3H; Trp NH_3); ^{13}C NMR: δ = 14.3, 21.5, 22.8, 25.7, 26.2, 28.3, 29.1, 31.9, 32.6, 53.6, 66.7, 105.3, 109.6, 118.6, 119.2, 121.7, 126.2, 127.7, 129.0, 130.0, 137.2, 140.5, 169.2 ppm.

Boc-GW(N-CHO)-OC_7H_{15}: TsOH·W(N-CHO)-OC_7H_{15} (0.65 g, 1.33 mmol), Boc-Gly-OH (0.23 g, 1.33 mmol), EDCI (0.28 g, 1.46 mmol), and HOBt (0.20 g, 1.46 mmol) were dissolved in CH_2Cl_2 (35 mL), cooled at 0 °C and Et_3N (0.56 mL) was added. The mixture was stirred at RT for 24 h, the solvent was evaporated, and the residue was subjected to chromatography (silica gel, hexane/EtOAc = 2:1) to afford an oil (0.39 g, 62 %). ^{1}H NMR: δ = 0.88 (t, J = 6.2 Hz, 3H; CH_2CH_3), 1.27 (pseudo-s, 8H; $OCH_2CH_2(CH_2)_4CH_3$), 1.43 (s, 9H; $C(CH_3)_3$), 1.57 (quint, J = 6.3 Hz, 2H; $OCH_2CH_2(CH_2)_4CH_3$), 3.32 (d, J = 5.3 Hz, 2H; Trp CH_2), 3.96 (d, J = 5.3 Hz, 2H; Gly CH_2), 3.70–3.85 (m, 5H; Gly CH_2 and indole NCH_3), 3.95–4.15 (m, 2H; $OCH_2CH_2(CH_2)_4CH_3$), 4.90 (q, J = 6.1 Hz, 1H; Trp *CH*), 5.07 (brs, 1H; *NH*), 6.46–7.55 ppm (m, 6H; *CONH* and indole *CH*); ^{13}C NMR: δ = 14.2, 22.8, 25.9, 27.8, 28.4, 28.6, 29.0, 31.9, 32.9, 44.4, 53.3, 65.9, 80.3, 108.4, 109.5, 118.7, 119.4, 122.0, 127.7, 128.4, 137.1, 156.0, 169.1, 171.9 ppm.

Boc-GGW(N-CHO)-OC_7H_{15}: Boc-GW(N-CHO)-OC_7H_{15} (0.38 g, 0.80 mmol) was deprotected (4N HCl/dioxane, 2 h). HCl·GW(N-CH_3)-OC_7H_{15}, Boc-Gly-OH (0.14 g, 0.80 mmol), EDCI (0.17 g, 0.88 mmol), and HOBt (0.12 g, 0.88 mmol) were suspended in CH_2Cl_2 (30 mL), the mixture was cooled to 0 °C, and Et_3N (0.34 mL) was added. The mixture was stirred at RT for 40 h. Evaporation of the solvent and chromatography (silica gel, $CHCl_3$/MeOH = 98:2) afforded a viscous solid (0.24 g, 56 %). ^{1}H NMR: δ = 0.88 (t, J = 6.6 Hz, 3H; CH_2CH_3), 1.25 (pseudo-s, 8H; $OCH_2CH_2(CH_2)_4CH_3$), 1.44 (s, 9H; $C(CH_3)_3$), 1.50–1.63 (m, 2H; $OCH_2CH_2(CH_2)_4CH_3$), 3.20–3.35 (m, 2H; Trp CH_2), 3.64–3.78 (m, 5H; Gly CH_2 and indole NCH_3), 3.84–4.12 (m, 4H; Gly CH_2 and $OCH_2CH_2(CH_2)_4CH_3$), 4.85 (q, J = 6.2 Hz, 1H; Trp *CH*), 5.19 (brs, 1H; *NH*), 6.60–7.55 (m, 7H; *CONH* and indole *CH*). ^{13}C NMR: δ = 14.2, 22.7, 25.9, 27.6,

28.5, 28.6, 29.0, 31.8, 32.9, 43.0, 44.3, 53.4, 65.9, 80.5, 108.4, 109.6, 118.7, 119.3, 122.0, 127.9, 128.3, 137.1, 156.2, 168.5, 170.1, 171.9 ppm.

Boc-PGGW(N-CHO)-OC$_7$H$_{15}$: Boc-GGW(N-CHO)-OC$_7$H$_{15}$ (0.22 g, 0.41 mmol) was deprotected (4N HCl/dioxane, 2 h). HCl·GGW(N-CH$_3$)-OC$_7$H$_{15}$, Boc-Pro-OH (0.089 g, 0.41 mmol), EDCI (0.087 g, 0.46 mmol), and HOBt (0.062 g, 0.46 mmol) were suspended in CH_2Cl_2 (25 mL) and Et_3N (0.17 mL) was added. The mixture was stirred at RT for 24 h. Evaporation of the solvent and chromatography (silica gel, $CHCl_3$/MeOH = 98:2- 95:5) gave a viscous semi-solid (0.26 g, 98%). ^{1}H NMR: δ = 0.89 (t, J = 6.8 Hz, 3H; CH_2CH_3), 1.26 (pseudo-s, 8H; $OCH_2CH_2(CH_2)_4CH_3$), 1.43 (s, 9H; $C(CH_3)_3$), 1.48–1.61 (m, 2H; $OCH_2CH_2(CH_2)_4CH_3$), 1.82–2.20 (m, 4H; Pro $NCH_2CH_2CH_2$), 3.28 (d, J = 5.7 Hz, 2H; Trp CH_2), 3.34–3.55 (m, 2H; Pro $NCH_2CH_2CH_2$), 3.68–4.20 (m, 10H; Gly CH_2, indole NCH_3, $OCH_2CH_2(CH_2)_4CH_3$ and Pro *CH*), 4.83 (q, J = 6.2 Hz, 1H; Trp *CH*), 6.73–7.65 ppm (m, 8H; *CONH* and indole *CH*); ^{13}C NMR: δ = 14.2, 22.8, 24.9, 25.9, 27.6, 28.6, 29.1, 29.6, 29.9, 31.8, 32.9, 43.3, 47.5, 53.3, 60.9, 65.8, 81.0, 108.6, 109.5, 118.8, 119.2, 121.8, 128.1, 128.4, 137.0, 155.9, 168.8, 169.9, 171.9, 173.5 ppm.

$(C_{18}H_{37})_2$NCOOCH$_2$OCH$_2$CO-Gly-Gly-Gly-Pro-Gly-Gly-Trp(N-CHO)-OC$_7$H$_{15}$ (**13**): Boc-PGGW(N-CHO)-OC$_7$H$_{15}$ (0.43 g, 0.67 mmol) was deprotected in 4N HCl/dioxane for 2 h. HCl·PGGW(N-CHO)-OC$_7$H$_{15}$, $(C_{18}H_{37})_2$DGA-GGG-OH (0.54 g, 0.67 mmol), EDCI (0.14 g, 0.74 mmol) and HOBt (0.10 g, 0.74 mmol) were suspended in CH_2Cl_2 (25 mL). To this mixture cooled at 0°C, was added Et_3N (0.28 mL). The mixture was warmed to room temperature and stirred for 48 h. The solvent was evaporated and the residue was crystallized from MeOH. The crude product was further purified by column chromatography (silica gel, $CHCl_3$/MeOH = 95:5–90:10) and then recrystallized from MeOH to afford a white solid (0.34 g, 38%). M.p. 172–174°C; ^{1}H NMR ($CDCl_3$): δ = 0.88 (t, J = 6.6 Hz, 9H; CH_2CH_3), 1.18–1.40 (m, 68H; $NCH_2CH_2(CH_2)_{15}CH_3$ and $OCH_2CH_2(CH_2)_4CH_3$), 1.40–1.64 (m, 6H; $NCH_2CH_2(CH_2)_{15}CH_3$ and $OCH_2CH_2(CH_2)_4CH_3$), 1.88–2.23 (m, 4H; Pro $NCH_2CH_2CH_2$), 3.06 (brt, J = 6.8 Hz, 2H; $NCH_2CH_2(CH_2)_{15}CH_3$), 3.16–3.33 (m, 4H; $NCH_2CH_2(CH_2)_{15}CH_3$ and Trp CH_2), 3.40–3.70 (m, 2H; Pro $NCH_2CH_2CH_2$), 3.70–4.40 (m, 17H; Gly CH_2, Pro *CH*, $OCH_2CH_2(CH_2)_4CH_3$ and OCH_2CO), 4.77 (brq, J = 6.8 Hz, 1H; Trp *CH*), 7.30–9.40 ppm (m, 12H; *CONH*, indole *CH* and *CHO*); ^{13}C NMR ($CDCl_3$): δ = 14.2, 14.3, 22.8, 22.9, 25.4, 26.0, 27.1, 27.3, 27.8, 28.6, 29.1, 29.2, 29.5, 29.6, 29.8, 29.9, 30.0, 31.9, 32.1, 42.2, 43.2, 43.8, 46.6, 47.2, 52.3, 61.5, 66.2, 69.6, 71.6, 116.3, 118.1, 118.8, 124.5, 124.8, 125.3, 131.4, 134.4, 160.6, 168.8, 169.1, 170.2, 170.3, 170.4, 170.7, 171.4, 172.0, 173.8 ppm; elemental analysis calcd (%) for $C_{74}H_{125}N_9O_{12}$: C 66.68, H 9.45, N 9.46; found: C 66.90, H 9.19, N 9.28.

$(C_{18}H_{37})_2$NCOOCH$_2$OCH$_2$CO-Gly-Gly-Gly-Pro-Gly-Gly-Trp-OC$_7$H$_{15}$ (**12**): Compound **13** (140 mg, 0.10 mmol) was dissolved in THF (7.5 mL). NaOH solution (1.5 mL, 0.1M aq.) was added dropwise to stirred solution. The mixture was stirred at RT for 40 min. TLC ($CHCl_3$:MeOH = 90:10) indicated complete transformation. Acetic acid (glacial) was added to adjust to pH 5–6 and the solvents were evaporated in vacuo. The residue was purified by column chromatography (silica gel, $CHCl_3$/MeOH = 93:7). Recrystallization from MeOH afforded a white solid (100 mg, 73%). M.p. 118–120°C; ^{1}H NMR ($CDCl_3$): δ = 0.80–1.00 (m, 9H; CH_2CH_3), 1.18–1.40 (m, 68H; $NCH_2CH_2(CH_2)_{15}CH_3$ and $OCH_2CH_2(CH_2)_4CH_3$), 1.49 (pseudo-s, 4H; $NCH_2CH_2(CH_2)_{15}CH_3$), 1.62 (brt, J = 6.8 Hz, 2H; $OCH_2CH_2(CH_2)_4CH_3$), 1.72–2.18 (m, 4H; Pro $NCH_2CH_2CH_2$), 3.03 (brt, J = 6.8 Hz, 2H; $NCH_2CH_2(CH_2)_{15}CH_3$), 3.14–3.34 (m, 4H; $NCH_2CH_2(CH_2)_{15}CH_3$ and Trp CH_2), 3.40–4.30 (m, 19H; Pro $NCH_2CH_2CH_2$, Gly CH_2, Pro *CH*, $OCH_2CH_2(CH_2)_4CH_3$ and OCH_2CO), 4.74 (brq, J = 7.3 Hz, 1H; Trp *CH*), 7.00–7.20 (m, 3H; indole *CH*), 7.30–7.60 (m, 4H; indole *CH* and *CONH*), 7.78–7.95 (m, 2H; *CONH*), 8.01 (brs, 1H; *CONH*), 8.21 (bt, J = 7.3 Hz, 1H; *CONH*), 9.53 ppm (s, 1H; indole *NH*); ^{13}C NMR ($CDCl_3$): δ = 14.2, 14.3, 22.8, 22.9, 25.2, 26.0, 27.1, 27.3, 27.6, 27.8, 28.7, 29.0, 29.1, 29.2, 29.5, 29.6, 29.8, 29.9, 31.9, 32.1, 41.9, 42.9, 43.4, 46.6, 46.9, 47.1, 53.0, 61.3, 66.0, 69.6, 71.4, 109.4, 111.8, 118.2, 119.1, 121.7, 124.6, 127.4, 136.5, 168.7, 168.9, 170.3, 170.4, 170.5, 171.2, 172.5, 173.5 ppm; IR ($CHCl_3$): $\tilde{\nu}$ = 3303, 3078, 2923, 2854, 1741, 1661, 1645, 1548, 1460, 1377, 1340, 1238, 1209, 1130, 1028 cm^{-1}; elemental analysis calcd (%) for $C_{73}H_{125}N_9O_{11}$: C 67.20, H 9.66, N 9.66; found: C 67.44, H 9.53, N 9.41.

Compound 14

N-*Methyl* L-*tryptophan* n-*heptyl ester tosylate*: A mixture of L-Trp(N-CH$_3$)-OH (0.60 g, 2.75 mmol), TsOH·H$_2$O (0.58 g, 3.02 mmol), 1-heptanol (3.1 mL, 22.0 mmol) and toluene (40 mL) was heated to reflux (10 h, Dean–Stark trap). The mixture was cooled to RT, Et_2O (200 mL) was added and the mixture was maintained at 0°C for 16 h. The solid product was collected by filtration (0.78 g, 58%). ^{1}H NMR: δ = 0.88 (t, J = 6.9 Hz, 3H; CH_2CH_3), 1.00–1.45 (m, 10H; $OCH_2(CH_2)_5CH_3$), 2.31 (s, 3H; $CH_3C_6H_4SO_3$), 3.30–3.40 (m, 2H; Trp CH_2), 3.49 (s, 3H; indole NCH_3), 3.73–3.98 (m, 3H; $OCH_2CH_2(CH_2)_4CH_3$ and Trp *CH*), 6.96–7.30 (m, 6H; indole *CH* and H_{Ar}), 7.42 (d, J = 7.8 Hz, 1H; indole *CH*), 7.60 (d, J = 7.8 Hz, 2H; H_{Ar}), 8.13 ppm (brs, 3H; Trp NH_3); ^{13}C NMR: δ = 14.3, 21.5, 22.8, 25.7, 26.2, 28.3, 29.1, 31.9, 32.6, 53.6, 66.7, 105.3, 109.6, 118.6, 119.2, 121.7, 126.2, 127.7, 129.0, 130.0, 137.2, 140.5, 169.2 ppm.

Boc-GW(N-CH$_3$)-OC$_7$H$_{15}$: TsOH·W(*N*-CH$_3$)-OC$_7$H$_{15}$ (0.65 g, 1.33 mmol), Boc-Gly-OH (0.23 g, 1.33 mmol), EDCI (0.28 g, 1.46 mmol), and HOBt (0.20 g, 1.46 mmol) were dissolved in CH_2Cl_2 (35 mL), cooled at 0°C, and Et_3N (0.56 mL) was added. The mixture was stirred at RT for 24 h. Evaporation of the solvent and chromatography (silica gel, hexane/EtOAc = 2:1) afforded an oil (0.39 g, 62%). ^{1}H NMR: δ = 0.88 (t, J = 6.2 Hz, 3H; CH_2CH_3), 1.27 (pseudo-s, 8H; $OCH_2CH_2(CH_2)_4CH_3$), 1.43 (s, 9H; $C(CH_3)_3$), 1.57 (quint, J = 6.3 Hz, 2H; $OCH_2CH_2(CH_2)_4CH_3$), 3.32 (d, J = 5.3 Hz, 2H; Trp CH_2), 3.96 (d, J = 5.3 Hz, 2H; Gly CH_2), 3.70–3.85 (m, 5H; Gly CH_2 and indole NCH_3), 3.95–4.15 (m, 2H; $OCH_2CH_2(CH_2)_4CH_3$), 4.90 (q, J = 6.1 Hz, 1H; Trp *CH*), 5.07 (brs, 1H; *NH*), 6.46–7.55 ppm (m, 6H; *CONH* and indole *CH*); ^{13}C NMR: δ = 14.2, 22.8, 25.9, 27.8, 28.4, 28.6, 29.0, 31.9, 32.9, 44.4, 53.3, 65.9, 80.3, 108.4, 109.5, 118.7, 119.4, 122.0, 127.7, 128.4, 137.1, 156.0, 169.1, 171.9 ppm.

Boc-GGW(N-CH$_3$)-OC$_7$H$_{15}$: Boc-GW(*N*-CH$_3$)-OC$_7$H$_{15}$ (0.38 g, 0.80 mmol) was deprotected (4N HCl/dioxane, 2 h). HCl·GW(N-CH$_3$)-OC$_7$H$_{15}$, Boc-Gly-OH (0.14 g, 0.80 mmol), EDCI (0.17 g, 0.88 mmol), and HOBt (0.12 g, 0.88 mmol) were suspended in CH_2Cl_2 (30 mL), cooled to 0°C, and Et_3N (0.34 mL) was added. The mixture was stirred at for 40 h. Evaporation of the solvent and chromatography (silica gel, $CHCl_3$/MeOH = 98:2) afforded a viscous semi-solid (0.24 g, 56%). ^{1}H NMR: δ = 0.88 (t, J = 6.6 Hz, 3H; CH_2CH_3), 1.25 (pseudo-s, 8H; $OCH_2CH_2(CH_2)_4CH_3$), 1.44 (s, 9H; $C(CH_3)_3$), 1.50–1.63 (m, 2H; $OCH_2CH_2(CH_2)_4CH_3$), 3.20–3.35 (m, 2H; Trp CH_2), 3.64–3.78 (m, 5H; Gly CH_2 and indole NCH_3), 3.84–4.12 (m, 4H; Gly CH_2 and $OCH_2CH_2(CH_2)_4CH_3$), 4.85 (q, J = 6.2 Hz, 1H; Trp *CH*), 5.19 (brs, 1H; *NH*), 6.60–7.55 ppm (m, 7H; *CONH* and indole *CH*); ^{13}C NMR: δ = 14.2, 22.7, 25.9, 27.6, 28.5, 28.6, 29.0, 31.8, 32.9, 43.0, 44.3, 53.4, 65.9, 80.5, 108.4, 109.6, 118.7, 119.3, 122.0, 127.9, 128.3, 137.1, 156.2, 168.5, 170.1, 171.9 ppm.

Boc-PGGW(N-CH$_3$)-OC$_7$H$_{15}$: Boc-GGW(*N*-CH$_3$)-OC$_7$H$_{15}$ (0.22 g, 0.41 mmol) was deprotected in 4N HCl/dioxane for 2 h. HCl·GGW(N-CH$_3$)-OC$_7$H$_{15}$, Boc-Pro-OH (0.089 g, 0.41 mmol), EDCI (0.087 g, 0.46 mmol), and HOBt (0.062 g, 0.46 mmol) were suspended in CH_2Cl_2 (25 mL) and Et_3N (0.17 mL) was added. The mixture was stirred at RT for 24 h. Evaporation of the solvent and chromatography (silica gel, $CHCl_3$/MeOH = 98:2- 95:5) gave a viscous semi-solid (0.26 g, 98%). ^{1}H NMR: δ = 0.89 (t, J = 6.8 Hz, 3H; CH_2CH_3), 1.26 (pseudo-s, 8H; $OCH_2CH_2(CH_2)_4CH_3$), 1.43 (s, 9H; $C(CH_3)_3$), 1.48–1.61 (m, 2H; $OCH_2CH_2(CH_2)_4CH_3$), 1.82–2.20 (m, 4H; Pro $NCH_2CH_2CH_2$), 3.28 (d, J = 5.7 Hz, 2H; Trp CH_2), 3.34–3.55 (m, 2H; Pro $NCH_2CH_2CH_2$), 3.68–4.20 (m, 10H; Gly CH_2, indole NCH_3, $OCH_2CH_2(CH_2)_4CH_3$ and Pro *CH*), 4.83 (q, J = 6.2 Hz, 1H; Trp *CH*), 6.73–7.65 ppm (m, 8H; *CONH* and indole *CH*); ^{13}C NMR: δ = 14.2, 22.8, 24.9, 25.9, 27.6, 28.6, 29.1, 29.6, 29.9, 31.8, 32.9, 43.3, 47.5, 53.3, 60.9, 65.8, 81.0, 108.6, 109.5, 118.8, 119.2, 121.8, 128.1, 128.4, 137.0, 155.9, 168.8, 169.9, 171.9, 173.5 ppm.

$(C_{18}H_{37})$NCOOCH$_2$OCH$_2$CO-Gly-Gly-Gly-Pro-Gly-Gly-Trp(N-CH$_3$)-OC$_7$H$_{15}$ (**14**): Boc-PGGW(*N*-CH$_3$)-OC$_7$H$_{15}$ (0.25 g, 0.40 mmol) was deprotected (4N HCl/dioxane, 2 h). HCl·PGGW(N-CH$_3$)-OC$_7$H$_{15}$, $(C_{18}H_{37})_2$NCOCH$_2$OCH$_2$CO-GGG-OH (0.32 g, 0.40 mmol), EDCI (0.084 g, 0.44 mmol), and HOBt (0.059 g, 0.44 mmol) were suspended in CH_2Cl_2 (20 mL). The mixture was cooled (0°C) and Et_3N (0.17 mL) was added. The mixture was stirred at RT for 60 h. The solvent was evaporat-

ed, the residue was crystallized (MeOH), and then subjected to chromatography (silica gel, $CHCl_3$/MeOH = 93:7–90:10). Crystallization from MeOH gave an off-white solid (0.27 g, 51 %). ^{1}H NMR: $\delta = 0.88$ (t, $J =$ 7.0 Hz, 9H; CH_2CH_3), 1.05–1.60 (m, 74H; $NCH_2(CH_2)_{16}CH_3$ and OCH_2-$(CH_2)_5CH_3$), 1.90–2.23 (m, 4H; Pro $NCH_2CH_2CH_2$), 3.98–3.34 (m, 6H; $NCH_2CH_2(CH_2)_{15}CH_3$ and Trp CH_2), 3.42–3.70 (m, 2H; Pro $NCH_2CH_2CH_2$), 3.72–4.18 (m, 17H; indole NCH_3, Gly CH_2, OCH_2CH_2-$(CH_2)_4CH_3$ and OCH_2CO), 4.20–4.37 (m, 3H; Pro *CH* and OCH_2CO), 4.62 (q, $J = 6.3$ Hz, 1H; Trp *CH*), 7.00–7.15 (m, 2H; indole *CH*), 7.17–7.30 (m, 3H; indole *CH* and *CONH*), 7.45–7.60 (m, 2H; indole *CH* and *CONH*), 7.86–8.03 (m, 3H; *CONH*), 8.39 ppm (brt, $J = 7.3$ Hz, 1H; *CONH*); ^{13}C NMR: $\delta = 14.2$, 14.3, 22.8, 22.9, 25.4, 25.9, 27.1, 27.3, 27.4, 27.8, 28.6, 29.0, 29.1, 29.2, 29.5, 29.6, 29.7, 29.8, 29.9, 31.9, 32.8, 42.1, 43.0, 43.1, 43.2, 43.7, 46.7, 47.1, 47.2, 53.8, 61.5, 65.9, 69.7. 71.6, 108.8, 109.5, 118.6, 119.1, 121.7, 128.0, 128.4, 137.1, 168.9, 169.1, 170.1, 170.2, 170.4, 170.5, 171.5, 172.6, 173.5 ppm. elemental analysis calcd (%) for $C_{74}H_{127}N_9O_{11}$: C 67.39, H 9.71, N 9.56; found: C 67.05, H 9.47, N 9.38.

Langmuir trough studies: HPLC grade $CHCl_3$ (Aldrich) was used to prepare amphiphile solutions with a concentration of about 1 mg mL^{-1} as determined by mass. Surface pressure-area isotherm experiments were carried out on a Langmuir trough (Nima, UK). Pressure was measured with a Wilhelmy plate made out of filter paper. Subphase temperature was maintained at (23.0 ± 0.1) °C by an Isotemp 3016 circulating thermostat. The subphase contained ultrapure water with a resistivity of 18.2 mW (Millipore). Monolayers were formed by spreading of solutions of compounds **1**–**5** (1.0 mg mL^{-1}) in $CHCl_3$ (50 mL) onto the subphase and allowing 10 min for the solvent to evaporate. Trough barriers were compressed at a constant speed of < 0.3 nm^2 mlc^{-1} min^{-1}. Data were plotted as surface pressure (mN m^{-1}) versus molecular area (Å^2). Isotherm data were collected in triplicate on each of four separate days, resulting in a total of 12 individual trials for each compound to obtain accurate isotherm information.

Dynamic light scattering: An approximate 1 mg mL^{-1} stock solution was prepared in HPLC grade hot 2-propanol. Between 20–200 μL of the solution was added to H_2O (2 mL, Millipore, 18 MΩ) to a glass culture tube (16 × 100 mm) and sonicated (Branson 1510 sonicator) at RT for 1.0 min. The aqueous solutions were then transferred by pipette to a BISCP square, polystyrene cuvette, 10 mm in length, 4.5 mL in volume (Brookhaven instruments). Dynamic light scattering measurements were performed on a 90Plus/BI-MAS multi angle particle sizing instrument from Brookhaven instruments (15 mW laser). Data were collected at (25 ± 0.03) °C. Scattered light was sampled at 90°. Each trial consisted of 4 runs lasting 3 min per run, on thin shells mode, with a dust cutoff of 100. Each sample was measured three times on at least two different days, and the effective diameters are an average of at least six trials. Particle size distributions as determined by intensity were also recorded.

Transmission electron microscopy: TEM was performed on a JEOL JEM 2000 FX electron microscope operating at 200 kV. A GATAN CCD camera was used to digitize the images. TEM samples were prepared as described above for dynamic light scattering. After sonication, a copper grid coated with lacey carbon on formvar, 300 mesh (Ted Pella Inc.), was dipped into the culture tube containing a solution of **4** and the water was allowed to evaporate. Because the solution was dilute, this process was repeated every 20 min for 2 h. After the dipping process was complete and the carbon film was completely dry, the film was placed on a single tilt sample holder and the images were collected.

Planar bilayer voltage clamp studies: Planar bilayer conductance measurements were performed with a Warner bilayer clamp instrument. Membranes were formed by painting lipid solutions (asolectin from soybean dissolved in decane, 25 mg mL^{-1}) over a 200 μm aperture separating two buffer filled (450 mM KCl, 10 mM HEPES, pH 7.00) chambers. A solution of the compound being studied was then added into the cis-chamber (the side of the membrane that hosts the input electrode) to make the final concentration of 2 μM. Specific potentials were applied between two electrodes immersed in two buffer solutions to record the currents in Faraday cage (from Warner Instruments, LLC). The currents were amplified (amplifier BC-525 D, from Warner Instruments, LLC), filtered with a 4-pole Bessel filter at 1 kHz, digitized by Digitizer (Digidata 1322 A from Axon Instruments), sampled at the 100 Hz of amplifier filter frequency and collected by Clampex 9.2 (software from Axon Instruments). The data were analyzed later using Clampfit v. 9.2 (software from Axon Instruments).

Acknowledgements

We thank the NIH for a grant (GM-63190) and the NSF (CHE-0957535) for grants that supported this work. We also gratefully acknowledge the expertise of Dr. Dan Zhou and the resources of the MIST lab, Center for Nanoscience.

[1] a) K. Kavallieratos, C. M. Bertao, R. H. Crabtree, *J. Org. Chem.* **1999**, *64*, 1675–1683; b) S. Kubik, *Chem. Soc. Rev.* **2009**, *38*, 585–605; c) P. A. Gale, *Acc. Chem. Res.* **2011**, *44*, 216–226.

[2] a) M. J. Deetz, M. Shang, B. D. Smith, *J. Am. Chem. Soc.* **2000**, *122*, 6201–6207; b) K. E. Mitchell, T. Iwamoto, J. Tomich, L. C. Freeman, *Biochim. Biophys. Acta Biomembr.* **2000**, *1466*, 47–60; c) J. M. Boon, B. D. Smith, *Curr. Opin. Chem. Biol.* **2002**, *6*, 749–756; d) S. B. Suh, C. Cui, H. S. Son, J. S. U., Y. Won, K. S. Kim, *J. Phys. Chem. B* **2002**, *106*, 2061–2064; e) D. Yang, J. Qu, W. Li, Y.-H. Zhang, Y. Ren, D.-P. Wang, Y.-D. Wu, *J. Am. Chem. Soc.* **2002**, *124*, 12410–12411; f) S. Kubik, R. Kirchner, D. Nolting, J. Seidel, *J. Am. Chem. Soc.* **2002**, *124*, 12752–12760; g) J. M. Mahoney, R. A. Marshall, A. M. Beatty, B. D. Smith, S. Camiolo, P. A. Gale, *J. Supramol. Chem.* **2001**, *1*, 289–292; h) V. Sidorov, F. W. Kotch, J. L. Kuebler, Y. F. Lam, J. T. Davis, *J. Am. Chem. Soc.* **2003**, *125*, 2840–2841; i) B. D. Smith, T. N. Lambert, *Chem. Commun.* **2003**, 2261–2268; j) B. A. McNally, A. V. Koulov, B. D. Smith, J. B. Joos, A. P. Davis, *Chem. Commun.* **2005**, 1087–1089; k) J. L. Seganish, J. T. Davis, *Chem. Commun.* **2005**, 5781–5783; l) J. L. Sessler, D. An, W. S. Cho, V. Lynch, M. Marquez, *Chem. Commun.* **2005**, 540–542; m) S. Kubik, C. Reyheller, S. Stuewe, *J. Inclusion Phenom. Macrocyclic Chem.* **2005**, *52*, 137–187; n) J. L. Seganish, J. C. Fettinger, J. T. Davis, *Supramol. Chem.* **2006**, *18*, 257–264; o) J. L. Sessler, D. E. Gross, W. S. Cho, V. M. Lynch, F. P. Schmidtchen, G. W. Bates, M. E. Light, P. A. Gale, *J Am Chem. Soc.* **2006**, *128*, 12281–12288; p) A. P. Davis, D. N. Sheppard, B. D. Smith, *Chem. Soc. Rev.* **2007**, *36*, 348–357; q) D. S. Kim, V. M. Lynch, K. A. Nielsen, C. Johnsen, J. O. Jeppesen, J. L. Sessler, *Anal. Bioanal. Chem.* **2009**, *395*, 393–400; r) D. W. Yoon, D. E. Gross, V. M. Lynch, C. H. Lee, P. C. Bennett, J. L. Sessler, *Chem. Commun.* **2009**, 1109–1111; s) G. W. Gokel, N. Barkey, *New J. Chem.* **2009**, *33*, 947–963.

[3] a) R. Dutzler, E. B. Campbell, M. Cadene, B. T. Chait, R. MacKinnon, *Nature* **2002**, *415*, 287–294; b) R. Dutzler, E. B. Campbell, R. MacKinnon, *Science* **2003**, *300*, 108–112; c) C. Miller, *Nature* **2006**, *440*, 484–489.

[4] T. M. Fyles, T. D. James, K. C. Kaye, *J. Am. Chem. Soc.* **1993**, *115*, 12315–12321.

[5] G. W. Gokel, P. H. Schlesinger, N. K. Djedovic, R. Ferdani, E. C. Harder, J. Hu, W. M. Leevy, J. Pajewska, R. Pajewski, M. E. Weber, *Bioorg. Med. Chem.* **2004**, *12*, 1291–1304.

[6] a) B. G. Cox, H. Schneider, *Coordination and Transport Properties of Macrocyclic Compounds in Solution*, Elsevier, Amsterdam, **1992**, p. 420; b) T. M. Fyles, *Chem. Soc. Rev.* **2007**, *36*, 335–347; c) J. T. Davis, O. Okunola, R. Quesada, *Chem. Soc. Rev.* **2010**, *39*, 3843–3862; d) S. Matile, A. Vargas Jentzsch, J. Montenegro, A. Fin, *Chem. Soc. Rev.* **2011**, *40*, 2453–2474; e) J. K. Chui, T. M. Fyles, *Chem. Soc. Rev.* **2012**, *41*, 148.

[7] P. Schlieper, E. De Robertis, *Arch. Biochem. Biophys.* **1977**, *184*, 204–208.

[8] T. K. Rostovtseva, C. L. Bashford, A. A. Lev, C. A. Pasternak, *J. Membr. Biol.* **1994**, *141*, 83–90.

[9] E. K. Elliott, K. J. Stine, G. W. Gokel, *J. Membr. Sci.* **2008**, *321*, 43–50.

[10] a) X. Li, B. Shen, X.-Q. Yao, D. Yang, *J. Am. Chem. Soc.* **2007**, *129*, 7264–7265; b) X. Li, Y. D. Wu, D. Yang, *Acc. Chem. Res.* **2008**, *41*,

1428–1438; c) X. Li, B. Shen, X.-Q. Yao, D. Yang, *J. Am. Chem. Soc.* **2009**, *131*, 13676–13680.
[11] D. Liu, S. Choi, B. Chen, R. J. Doerksen, D. J. Clements, J. D. Winkler, M. L. Klein, W. F. DeGrado, *Angew. Chem. Int. Ed.* **2004**, *43*, 1158–1162.
[12] N. Sakai, D. Houdebert, S. Matile, *Chem. Eur. J.* **2003**, *9*, 223–232.
[13] T. M. Fyles, H. Luong, *Org. Biomol. Chem.* **2009**, *7*, 733–738.
[14] Y. Shai, *Curr. Pharm. Des.* **2002**, *8*, 715–725.
[15] L. You, G. W. Gokel, *Chem. Eur. J.* **2008**, *14*, 5861–5870.
[16] D. Voet, J. G. Voet, *Biochemistry Vol 1.*, 3rd ed., Wiley, Hoboken, NJ, **2004**, p. 66.
[17] W.-M. Yau, W. C. Wimley, K. Gawrisch, S. H. White, *Biochemistry* **1998**, *37*, 14713–14718.
[18] E. K. Esbjörner, C. E. B. Caesar, B. Albinsson, P. Lincoln, B. Nordén, *Biochem. Biophys. Res. Commun.* **2007**, *361*, 645650.
[19] M. R. de Planque, B. B. Bonev, J. A. Demmers, D. V. Greathouse, R. E. Koeppe, F. Separovic, A. Watts, J. A. Killian, *Biochemistry* **2003**, *42*, 5341–5348.
[20] T. M. Weiss, P. C. van der Wel, J. A. Killian, R. E. Koeppe, 2nd; H. W. Huang, *Biophys. J.* **2003**, *84*, 379–385; H. W. Huang, *Biophys. J.* **2003**, *84*, 379–385.
[21] a) V. V. Andrushchenko, H. J. Vogel, E. J. Prenner, *Biochim. Biophys. Acta Biomembr.* **2007**, *1768*, 2447–2458; b) S. Persson, J. Antoinette Killian, G. Lindblom, *Biophys. J.* **1998**, *75*, 13651371; c) J. M. Sanderson, E. J. Whelan, *Phys. Chem. Chem. Phys.* **2004**, *6*, 1012–1017.
[22] a) K. E. Norman, H. Nymeyer, *Biophys. J.* **2006**, *91*, 2046; b) H. C. Gaede, W. M. Yau, K. Gawrisch, *J. Phys. Chem. B* **2005**, *109*, 13014.
[23] E. Abel, S. L. De Wall, W. B. Edwards, S. Lalitha, D. F. Covey, G. W. Gokel, *Chem. Commun.* **2000**, 433.
[24] N. Djedovič, R. Ferdani, E. Harder, J. Pajewska, R. Pajewski, M. E. Weber, P. H. Schlesinger, G. W. Gokel, *New J. Chem.* **2005**, *29*, 291–305.
[25] P. H. Schlesinger, R. Ferdani, J. Pajewska, R. Pajewski, G. W. Gokel, *New J. Chem.* **2003**, *27*, 60–67.
[26] R. Ferdani, G. W. Gokel, *Org. Biomol. Chem.* **2006**, *4*, 3746.
[27] a) V. Koulov, T. N. Lambert, R. Shukla, M. Jain, J. M. Boon, B. D. Smith, H. Li, D. N. Sheppard, J. B. Joos, J. P. Clare, A. P. Davis, *Angew. Chem.* **2003**, *115*, 5081; *Angew. Chem. Int. Ed.* **2003**, *42*, 4931; b) A. V. Koulov, J. M. Mahoney, B. D. Smith, *Org. Biomol. Chem.* **2003**, *1*, 27.
[28] P. H. Schlesinger, R. Ferdani, J. Liu, J. Pajewska, R. Pajewski, M. Saito, H. Shabany, G. W. Gokel, *J. Am. Chem. Soc.* **2002**, *124*, 1848–1849.
[29] L. You, R. Ferdani, R. Li, J. P. Kramer, R. E. Winter, G. W. Gokel, *Chem. Eur. J.* **2008**, *14*, 382–396.
[30] E. K. Elliott, M. M. Daschbach, G. W. Gokel, *Chem. Eur. J.* **2008**, *14*, 5871–5879.
[31] a) B. Hille, Ionic Channels of Excitable Membranes, 3rd ed.; Sinauer Associates: Sunderland, MA, **2001**; b) O. S. Smart, J. Breed, G. R. Smith, M. S. P. Sansom, *Biophys. J.* **1997**, *72*, 11091126.
[32] R. Pajewski, R. Ferdani, J. Pajewska, N. Djedovic, P. H. Schlesinger, G. W. Gokel, *Org. Biomol. Chem.* **2005**, *3*, 619–625.
[33] J. Zhou, X. Lu, Y. Wang, J. Shi, *Fluid Phase Equilib.* **2002**, *194–197*, 257–270.
[34] D. A. Doyle, J. M. Cabral, R. A. Pfuetzner, A. Kuo, J. M. Gulbis, S. L. Cohen, B. T. Chait, R. MacKinnon, *Science* **1998**, *280*, 69–77.
[35] "Gramicidin and Related Ion-Channel-Forming Peptides": *Novartis Found. Symp.* **1999**, *225*, whole volume.
[36] R. R. Ketchem, W. Hu, T. A. Cross, *Science* **1993**, *261*, 1457–1460.
[37] E. Abel, M. F. Fedders, G. W. Gokel, *J. Am. Chem. Soc.* **1995**, *117*, 1265–1270.
[38] S. K. Burley, G. A. Petsko, *FEBS Lett.* **1986**, *203*, 139–143.
[39] V. P. Santarelli, A. L. Eastwood, D. A. Dougherty, R. Horn, C. A. Ahern, *J. Biol. Chem.* **2007**, *282*, 8044–8051.
[40] M. E. Weber, E. K. Elliott, G. W. Gokel, *Org. Biomol. Chem.* **2006**, *4*, 83–89.
[41] G. A. Cook, R. Pajewski, M. Aburi, P. E. Smith, O. Prakash, J. M. Tomich, G. W. Gokel, *J. Am. Chem. Soc.* **2006**, *128*, 1633–1638.

Received: October 10, 2011
Revised: January 16, 2012
Published online: April 26, 2012

